WATER MOVEMENT IN NONISOTHERMAL TUFF

by

Bill Edward Davies

A Thesis Submitted to the Faculty of the

DEPARTMENT OF HYDROLOGY AND WATER RESOURCES

In Partial Fulfillment of the Requirements
For the Degree of

MASTER OF SCIENCE
WITH A MAJOR IN HYDROLOGY

In the Graduate College

THE UNIVERSITY OF ARIZONA

1 9 8 7

HYDROLOGY DOCUMENT NUMBER 470

CHAPTER 4

RESULTS OF LABORATORY COUNTERCURRENT EXPERIMENTS

Three laboratory heating experiments are analyzed in this section. The first two were performed on nonwelded tuff. The third experiment used a densely-welded tuff of similar chemical composition. The first core was heated in a vertical position. The second and third cores were orientated horizontally. Each core was heated for 32 days. Data will be presented showing the initial and steady-state water content distributions, the thermal gradients within the cores during heating, and the initial and final concentrations of a soluble tracer within the cores.

Nonwelded Tuff in a Vertical Position

In this experiment, a nonwelded tuff core, 12.72 cm in length and 6.4 cm in diameter, was heated under a constant thermal gradient. The dry bulk density of the core, found gravimetrically, was 2.12 gm/cm^3. Assuming a particle density of 2.65 gm/cm^3, the porosity was 0.20. The discrete bulk densities for twelve 1-cm intervals are given in Figure 4.1. These values were the result of three series of gamma measurements performed on the oven dried core. The average of these 12 measurements was 2.118 gm/cm^3 with a range between 2.074 and 2.158 gm/cm^3.

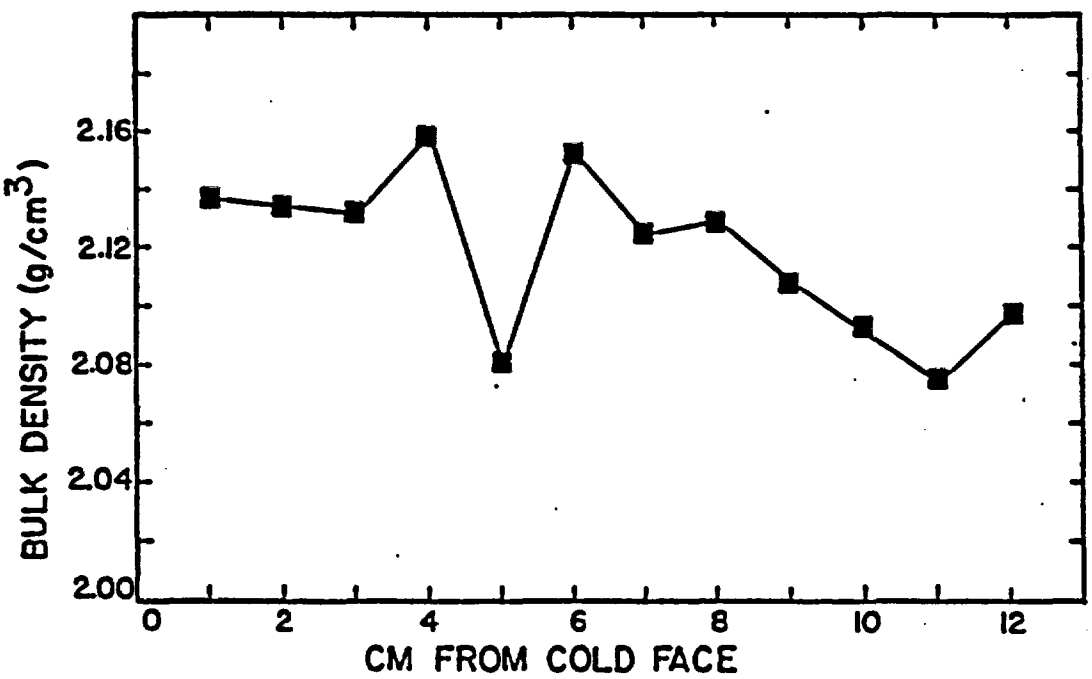

Figure 4.1 The dry bulk densities at twelve 1-cm intervals along the nonwelded tuff core used in the vertical heating experiment.

The core was wetted with a 1000 ppm solution of potassium iodide under a negative air pressure of approximately -85 centibars. The initial water content of the wetted core is shown in Figure 4.2. The core was put into a pressure chamber and allowed to equilibrate at different pressures to desaturate the core. The results of the desaturation are also shown in Figure 4.2. Gravimetric measurements indicated that less water loss occurred when the pressure in the chamber exceeded 1 bar. Evaporation during water content measurements also contributed to the water loss in the core. Data for Figure 4.2 are given in Table 4.1 along with gravimetric readings when taken.

After the core was brought to an intermediate level of saturation, approximately 41% saturation, it was sealed and attached to the heating apparatus. The sealant was not completely uniform and altered the gamma attenuation. Gamma measurements were retaken along the core and compared with the final water content readings taken before the core was sealed. The difference between the readings was found at each interval. This difference became an added term to equation [3.1] to account for the sealant attenuation. The assumption that no water movement occurred during the sealing process is made here.

The core was wrapped in foam insulation and subjected to a thermal gradient for 32 days. The hot and cold plate temperatures were approximately 69°C and 4°C, respectively, for an average thermal gradient of 5.1°C/cm (Fig. 4.3). The near steady-state thermal gradient was reached within 12 hours and remained nearly constant throughout the experiment except during the time when water content readings were taken

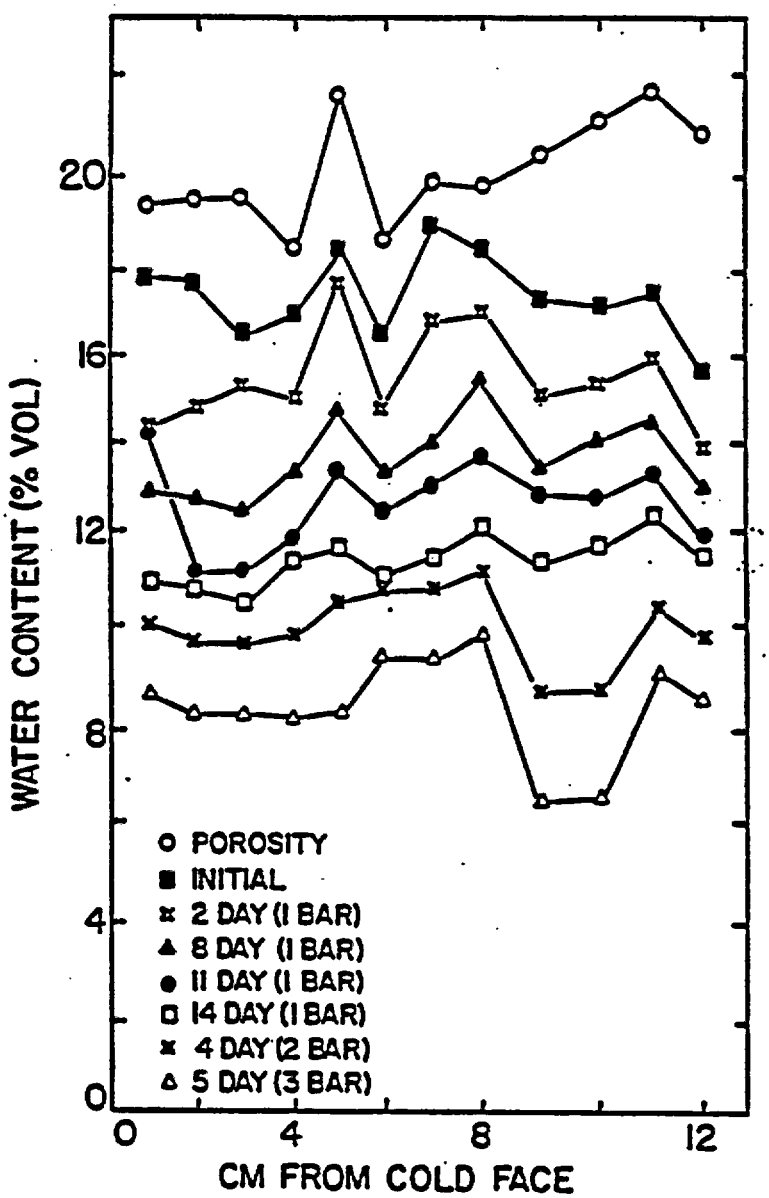

Figure 4.2 The initial, intermediate and final water content distributions within the nonwelded tuff core, used in the first heating experiment, being desaturated with a pressure plate. The time represents the amount of time the core was in the pressure plate at that particular pressure.

Cm from cold face	porosity	wetted core	46 hr 1 bar	188 hr 1 bar	260 hr 1 bar	332 hr 1 bar	96 hr 2 bar	48 hr 3 bar	120 hr 3 bar
1.00	19.36	17.90	14.34	12.88	14.16	10.75	10.01	9.65	8.60
2.00	19.47	17.62	14.81	12.72	11.16	10.64	9.65	9.02	8.32
3.00	19.55	16.47	15.31	12.45	11.13	10.31	9.61	8.90	8.31
4.00	18.57	17.03	15.07	13.38	11.86	11.34	9.74	9.74	8.24
5.00	21.51	19.53	17.55	14.71	13.26	11.55	10.48	9.48	8.31
6.00	18.79	16.47	14.74	13.33	12.49	11.05	10.80	10.64	9.45
7.00	19.85	18.96	16.83	14.02	13.13	11.40	10.80	10.48	9.41
8.00	19.66	18.47	16.99	15.46	13.72	12.12	11.17	11.15	9.62
9.00	20.49	17.27	15.14	13.14	12.48	10.91	8.62	8.20	7.43
10.00	21.02	16.81	15.42	14.06	12.40	11.27	8.69	8.39	7.49
11.00	21.74	17.21	15.62	14.48	13.33	12.05	10.39	10.43	9.20
12.00	20.87	15.71	13.84	12.96	11.85	11.43	9.76	9.86	8.47
Average	20.07	17.45	15.48	13.63	12.58	11.23	9.98	9.66	8.57
Gravimetric before gamma		19.20	NT	13.67	12.68	11.70	9.96	9.31	8.49
after gamma		NT	NT	NT	NT	11.31	9.81	9.26	8.24

NT = measurement not taken

Table 4.1 The data used in Figure 4.2 describing the desaturation of the nonwelded tuff core used in the first heatin experiment. The water content distributions were found with gamma attenuation are also averaged and compared to the gravimetric water content when that measurement was taken.

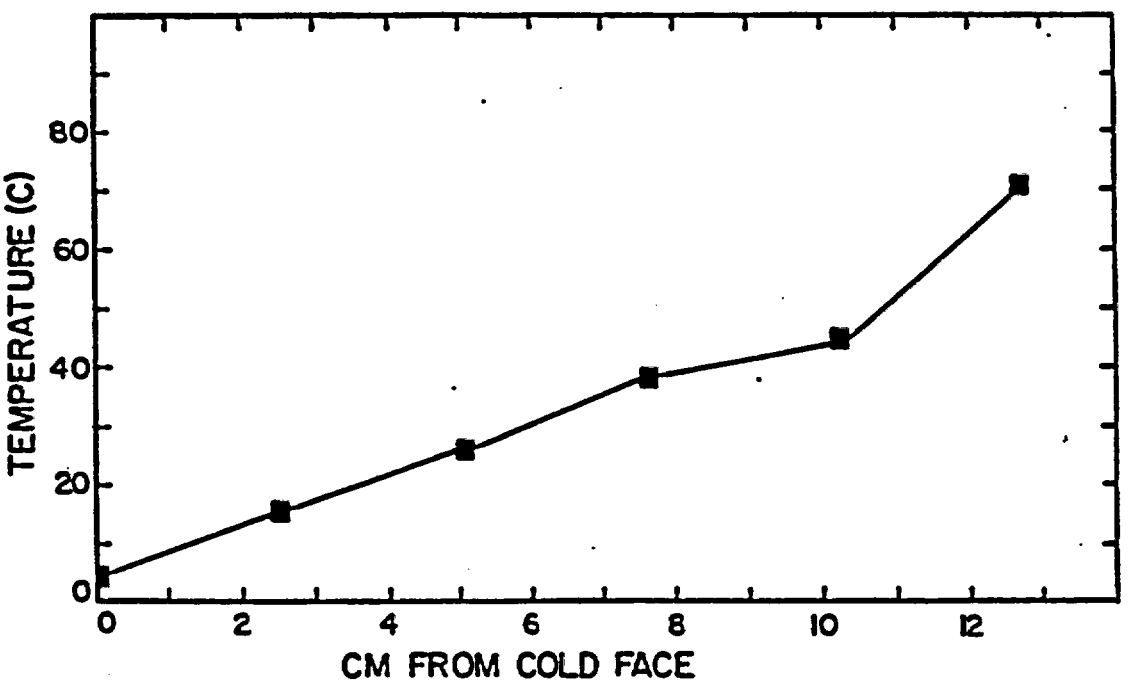

Figure 4.3 The temperature distribution within the nonwelded tuff core as it was heated in a vertical position.

and the insulation was removed. This deviation was slight and the temperature gradient recovered within 1 hour after replacing the fo For the first 36 hours, the core was in a horizontal position. The was then turned so that the cold face was down. The core remained this position for 17 days except when gamma measurements were taker this time, it appeared that the water content profile had reached a steady state. The core was then reoriented so that the hot face wa down. The position of the core was reversed to determine the effec gravity on the liquid return flow. The core remained in this posit for 13 days with no appreciable change in the water content profile (Fig. 4.4). The hot end of the core developed a crack in the epoxy days before the end of heating and some water loss was observed at end of the core. These results are not included in Figure 4.4. T 4.2 shows the change in water content, within the core, during hea

After heating, the core was sawed into 8 pieces with an oi cooled diamond saw. The amount of iodide in each section was det using high performance liquid chromatography. The results of thi analysis are reported in two ways: (1) The change in the amount iodide in each core section, and (2) The change in the concentra the solution inside each of the core sections. These data are g Table 4.3 and Figures 4.5 and 4.6. These results clearly show i movement toward the heat source.

Nonwelded Tuff in a Horizontal Position

This experiment was similar to the first experiment exc the core was heated in a horizontal position. The core was ta

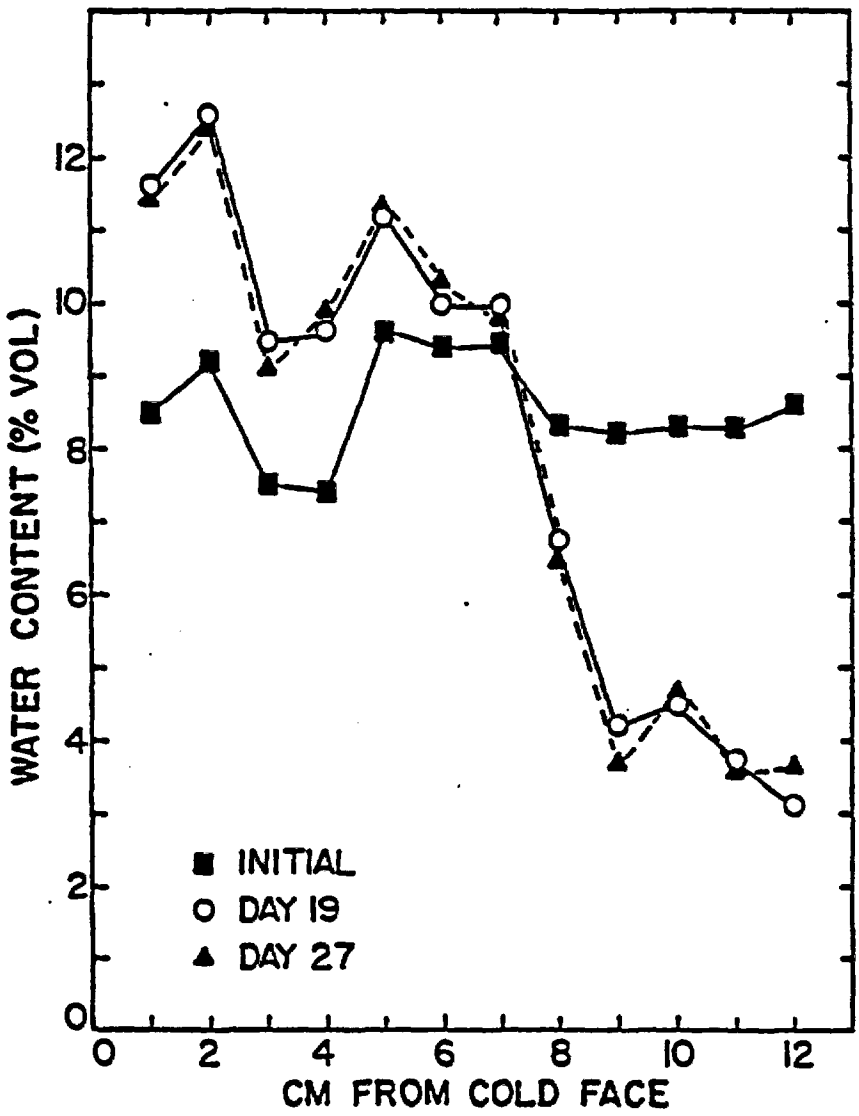

Figure 4.4 The initial, intermediate and final water content distributions within the nonwelded tuff core heated vertically. The core position was reversed after the 19th day of heating.

Table 4.2 Periodic water content measurements of the nonwelded tuff core during heating in a vertical position.

CM FROM COLD FACE	1.00	2.00	3.00	4.00	5.00	6.00	7.00	8.00	9.00	10.00	11.00	12.00	Ave.
Initial H2O Cont.	8.47	9.22	7.49	7.43	9.63	9.42	9.44	8.31	8.24	8.30	8.32	8.60	8.57
Time After Heating													
Cold Face Down													
Day 2	9.33	10.19	7.21	8.36	10.76	9.47	9.98	8.57	8.32	8.84	7.55	7.50	8.84
Day 3	10.57	10.31	7.21	8.54	10.62	9.67	10.08	8.05	8.11	8.00	7.10	5.13	8.63
Day 4	9.95	10.63	7.93	8.13	10.34	9.47	10.15	7.78	7.34	6.99	5.08	3.52	8.13
Day 6	11.22	11.50	8.22	8.70	10.71	10.04	9.62	7.61	7.56	6.34	4.85	3.64	8.35
Day 7	11.62	12.00	8.47	9.04	11.11	9.78	9.69	7.61	7.50	5.81	4.52	7.22	8.72
Day 9	11.26	12.02	9.14	8.47	10.67	9.64	9.92	7.07	6.16	4.62	3.81	2.75	7.98
Day 10	11.39	12.20	8.45	8.80	11.24	9.67	9.97	7.45	5.88	4.61	4.09	4.46	8.20
Day 12	11.21	12.58	9.04	9.29	11.00	9.67	10.23	7.44	6.75	5.16	3.80	5.59	8.66
Day 16	11.53	12.50	9.36	9.44	10.66	9.72	9.47	6.58	4.56	3.99	3.36	3.71	7.91
Day 18	11.71	12.46	9.29	9.61	11.15	9.93	10.03	7.07	4.31	4.65	3.93	4.02	8.18
Day 19	11.62	12.62	9.45	9.60	11.17	9.92	9.93	6.76	4.21	4.50	3.66	3.08	8.05
Hot Face Down													
Day 20	11.78	12.77	9.04	9.70	11.09	9.97	9.83	6.96	4.78	4.37	3.61	3.03	8.07
Day 23	11.99	12.42	8.62	9.61	11.14	9.91	9.69	6.73	4.08	4.24	3.66	3.10	7.93
Day 27	11.52	12.39	9.09	9.92	11.27	10.27	9.76	6.45	3.70	4.65	3.64	3.66	8.03
Leakage													
Day 31	11.52	12.70	7.66	9.40	10.65	9.77	9.37	5.58	2.97	3.43	2.56	1.67	7.32

Core section cm from cold side	0-1.74	1.74-3.3	3.3-4.8	4.8-6.16	6.16-7.8	7.8-9.65	9.65-11.1	11.1-12.79
Conc. I- (ppm)								
before heat	1000	1000	1000	1000	1000	1000	1000	1000
after heat	81	100	152	259	323	4746	5389	3830
Amount I- (mg/cm core)								
before heat	2.09	1.91	2	2.3	2.21	2	2.01	2.05
after heat	.23	.24	.38	.68	.67	5.28	5.64	3.37

Table 4.3 The results of the iodide analysis for the nonwelded tuff core heated vertically.

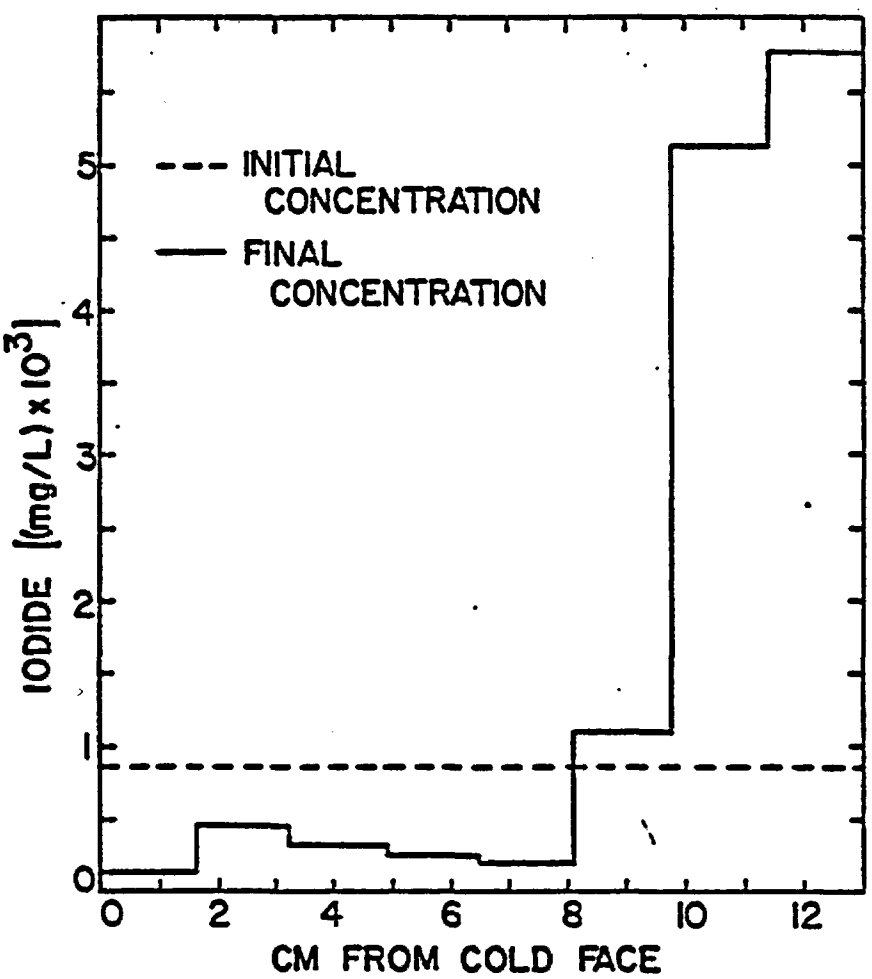

Figure 4.5 The change in concentration of iodide in the pore solution within the nonwelded tuff core heated vertically.

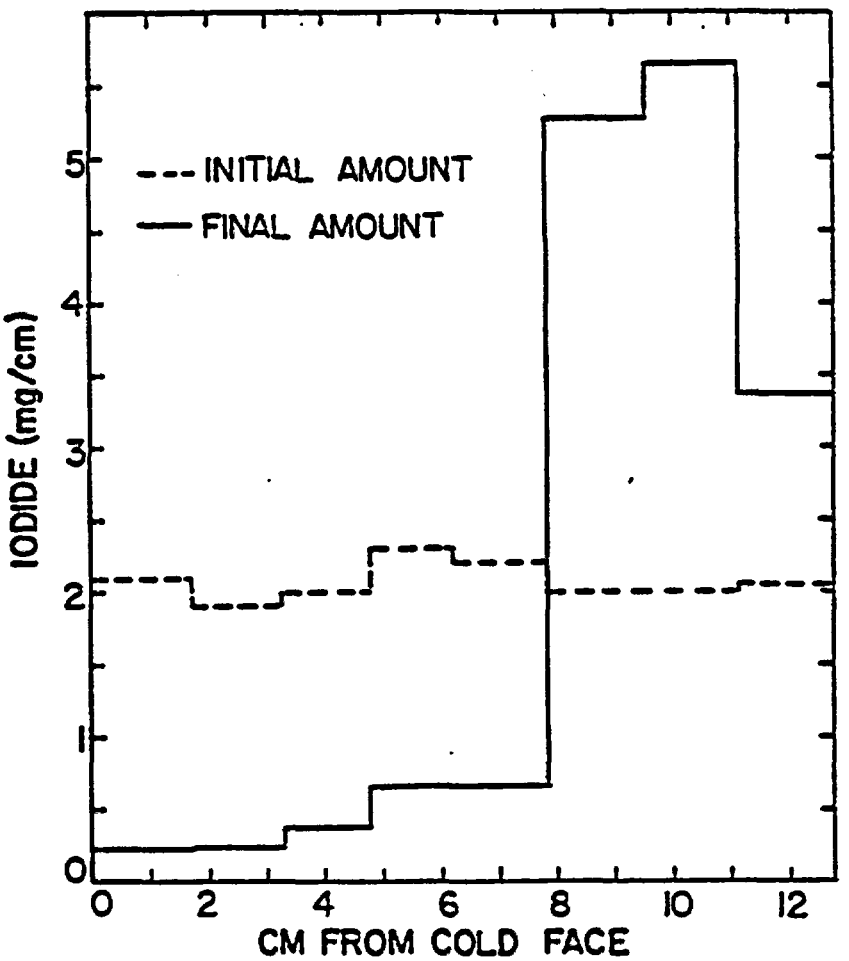

Figure 4.6 The change in the amount of iodide within each section of the nonwelded tuff core, which was heated vertically. All ion movement is assumed to be caused by liquid flow.

the same tuff zone and was approximately the same size as the tuff core used in the previous experiment. The temperatures in the hot and cold water reservoirs were similar to the first experiment, as was the amount of time the core was subjected to a thermal gradient. The core was 12.99 cm in length and 6.4 cm in diameter. The gravimetric bulk density was 2.15 gm/cm^3 giving a porosity of 0.19. This porosity is slightly lower than in the first experiment.

The core was initially wetted with a 1000 ppm solution of potassium iodide. Due to difficulties with the gamma equipment, the core was dried again and the bulk density measurements were retaken. The discrete bulk densities for twelve 1-cm intervals are given in Figure 4.7. These are the average of 5 series of gamma measurements. The average of these 12 measurements was 2.141 gm/cm^3 with a range between 2.108 and 2.166 gm/cm^3. Oven drying the core, after wetting with a potassium iodide solution, left some iodide in the core. When the core was rewetted, an 800 ppm solution was used. This was done in an attempt to approximate the original 1000 ppm solution. Analysis at the end of this experiment indicated that the solution within the core was approximately 875 ppm. The core was then desaturated and sealed in a similar manner as in the first experiment. The saturation level was approximately 48%. This saturation level was higher than the 41% saturation obtained in the first experiment.

The core was heated in a horizontal position for 32 days. Figure 4.8 shows the steady-state thermal gradient within the core. The temperature at the cold end in this figure is the cold fluid

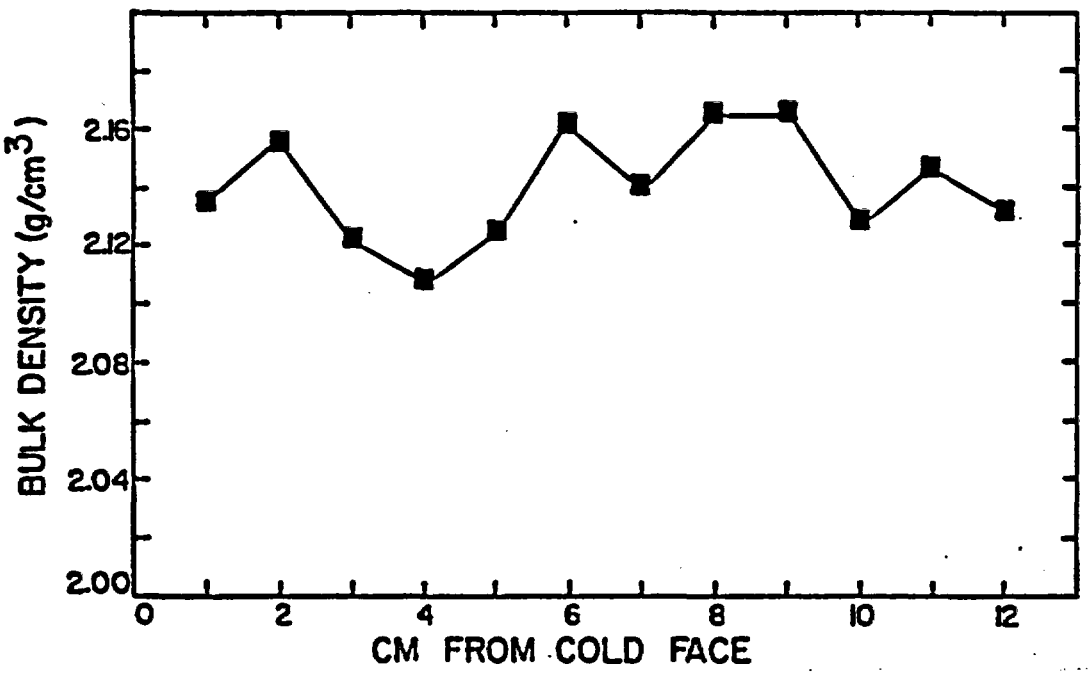

Figure 4.7 The dry bulk densities at twelve 1-cm intervals along the nonwelded tuff core, which was heated vertically.

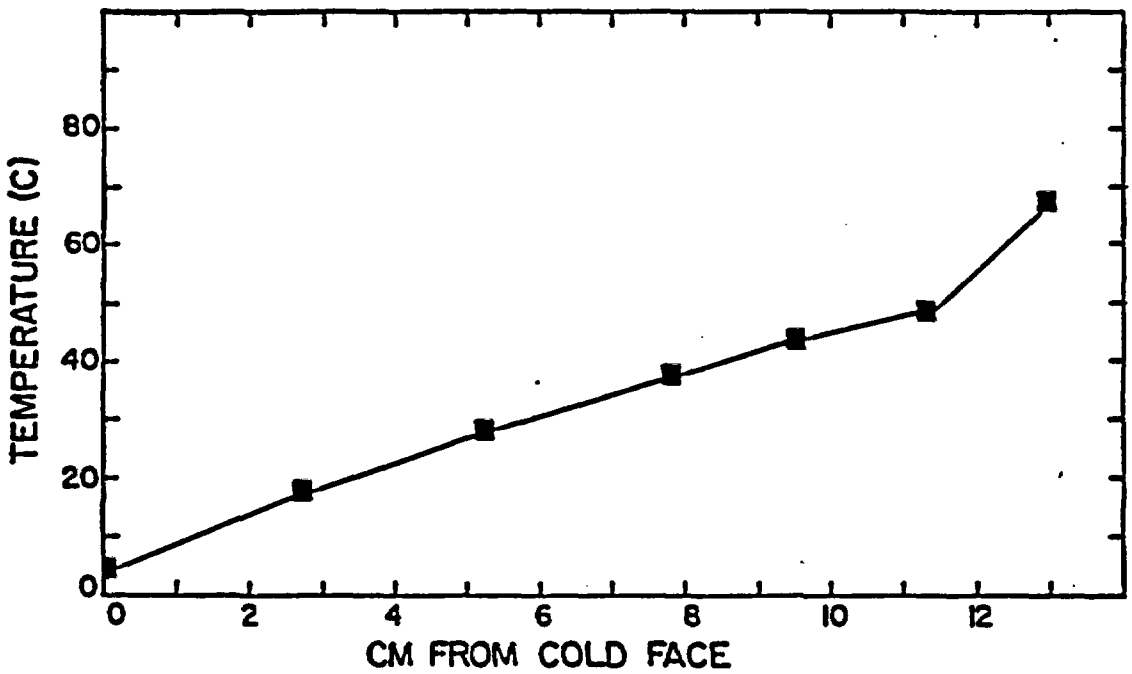

Figure 4.8 The temperature distribution within the nonwelded tuff core as it was heated in a horizontal position.

temperature. The temperature at the hot end of the core in this figure was measured by a thermocouple installed between the hot reservoir endplate and the core. The temperature between the core and the endplate was 67.2°C, while the hot fluid temperature was 69.8°C. The changes in water content were measured daily throughout the experiment. Figure 4.9 shows the initial and final water contents within the core. Data for the water movement within the core during heating are given in Table 4.4.

After the heating, the core was dissected into 16 pieces. The core was cut into 8 slices as in the previous experiment. These sections were then cut in half along a plane which separated the sections into upper and lower halves of the heated cylinder. The iodide analysis could then determine if more liquid return flow occurred along the bottom of the core than in the upper portion. The results of the iodide measurements are given in Table 4.5. These results do not indicate that more liquid water flowed along the bottom of the core. Figures 4.10 and 4.11 show the iodide movement within the core. An average of the analysis for the upper and lower portions of each core slice is used in these figures.

Welded Tuff in a Horizontal Position

In this experiment a densely-welded tuff core, with a larger diameter than the cores used in the previous experiments, was heated for 32 days at temperatures similar to the nonwelded tuff experiments. The dimensions of the core were 12.20 cm in length and 9.5 cm in diameter. The gravimetric bulk density of the core was 2.42 gm/cm^3 and the

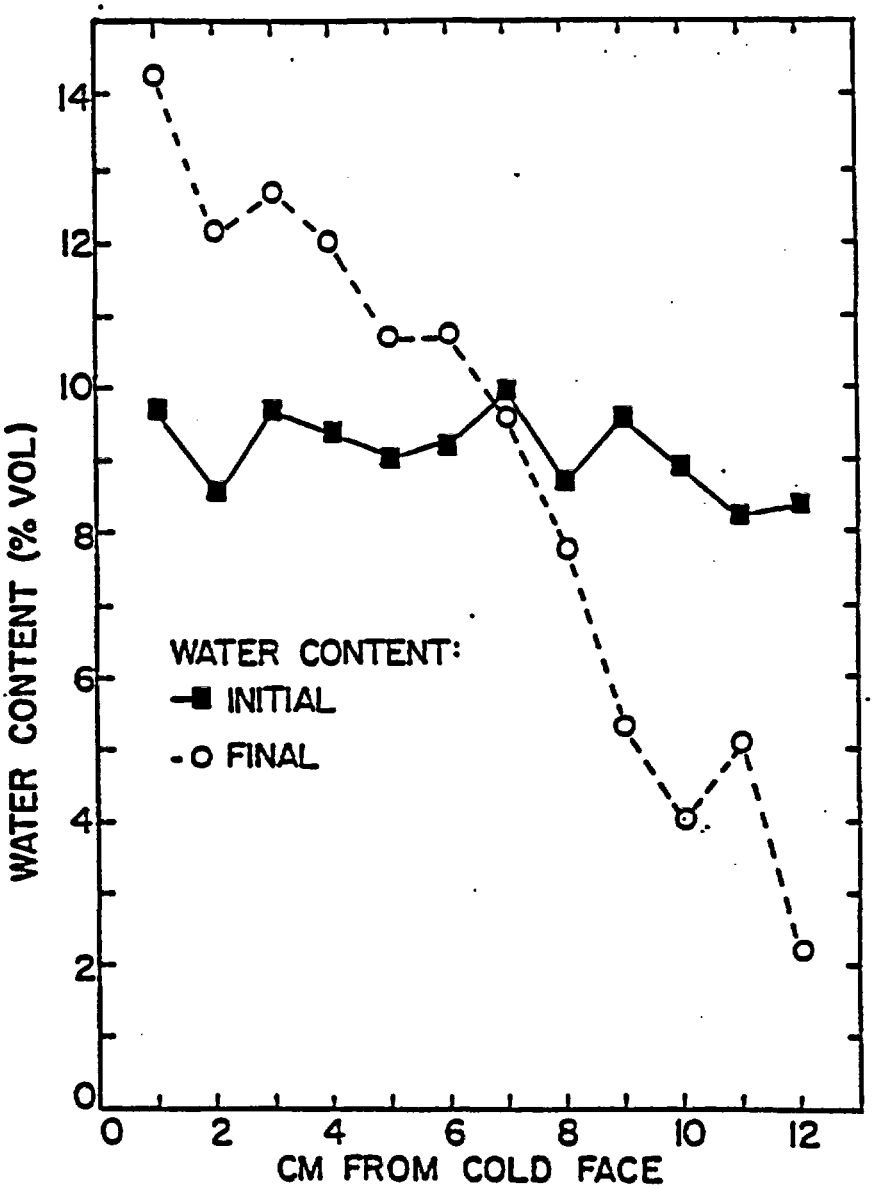

Figure 4.9 The initial and final water content of the nonwelded tuff core heated horizontally.

Table 4.4 Periodic water content measurements of the nonwelded tuff core heated horizontally.

CM FROM COLD FACE	1.00	2.00	3.00	4.00	5.00	6.00	7.00	8.00	9.00	10.00	11.00	12.00	Ave.
Initial H20 Cont.	9.69	8.58	9.70	9.38	9.04	9.23	9.99	8.71	9.60	8.94	8.25	8.40	9.13
Time After Heating													
Day 1	10.80	9.16	10.26	9.71	8.88	9.74	9.90	9.04	7.88	8.13	8.44	8.74	9.05
Day 3	11.34	10.06	10.88	10.45	9.37	10.22	9.93	8.64	7.33	7.53	7.60	5.93	9.09
Day 4	12.30	10.50	10.71	10.88	9.46	10.18	10.24	8.57	7.40	7.28	7.41	4.71	9.13
Day 5	12.77	10.75	11.34	10.82	9.36	9.83	10.22	8.39	6.94	7.05	6.89	4.66	9.09
Day 6	12.68	10.88	11.65	11.07	9.96	10.52	9.95	8.25	7.07	6.89	6.37	4.75	9.17
Day 7	13.07	10.91	12.05	11.17	9.90	10.43	10.19	8.58	6.61	7.00	6.45	3.96	9.19
Day 10	13.17	11.67	12.23	11.40	10.24	10.49	10.05	8.43	6.80	6.35	5.78	2.39	9.08
Day 11	13.78	11.93	12.20	11.78	10.34	10.60	10.18	8.71	6.58	6.21	5.61	2.45	9.20
Day 12	13.98	11.55	12.49	11.54	10.28	10.61	10.13	8.25	6.34	6.02	5.93	2.40	9.13
Day 14	14.14	11.95	12.43	11.74	10.36	10.75	9.95	8.38	6.63	5.57	5.64	2.35	9.16
Day 17	14.07	11.59	12.64	11.85	10.76	10.45	9.84	8.58	6.11	5.23	5.05	1.79	8.99
Day 19	14.06	11.93	12.55	12.04	10.89	10.81	10.18	8.05	6.09	5.06	5.18	2.28	9.08
Day 21	13.96	11.65	12.56	11.97	10.37	10.65	9.72	7.80	6.27	4.78	4.64	2.06	8.88
Day 27	14.04	12.03	12.90	12.25	10.55	11.04	10.19	7.35	5.81	4.40	5.30	2.11	8.98
Day 28	14.23	12.03	12.87	11.78	10.72	10.72	9.60	8.12	5.43	4.26	4.99	2.20	8.92
Day 30	14.26	12.17	12.73	12.05	10.71	10.75	9.81	7.78	5.31	4.00	5.15	2.17	8.89

Core section cm from cold side	0-1.57	1.57-3.1	3.1-4.8	4.8-6.57	6.57-8.04	8.04-9.8	9.8-11.3	11.3-12.89
Conc. I- (ppm)								
before heat	870	870	870	870	870	870	870	870
after heat								
upper half	170	482	261	225	269	1548	4911	5915
lower half	156	467	401	277	145	655	5357	5610
average	163	474	331	251	207	1101	5131	5762
Amount I-								
before heat	1.97	1.97	1.95	1.84	2.01	1.96	1.84	1.76
after heat								
upper half	.28	.73	.37	.29	.29	1.18	2.61	2.27
lower half	.26	.71	.56	.36	.16	.46	2.84	2.15
total	.54	1.44	.93	.65	.45	1.64	5.45	4.42

Table 4.5 The results of the iodide analysis of 16 core sections. Sections representing the upper and lower halves of the nonwelded tuff core heated horizontally were analyzed.

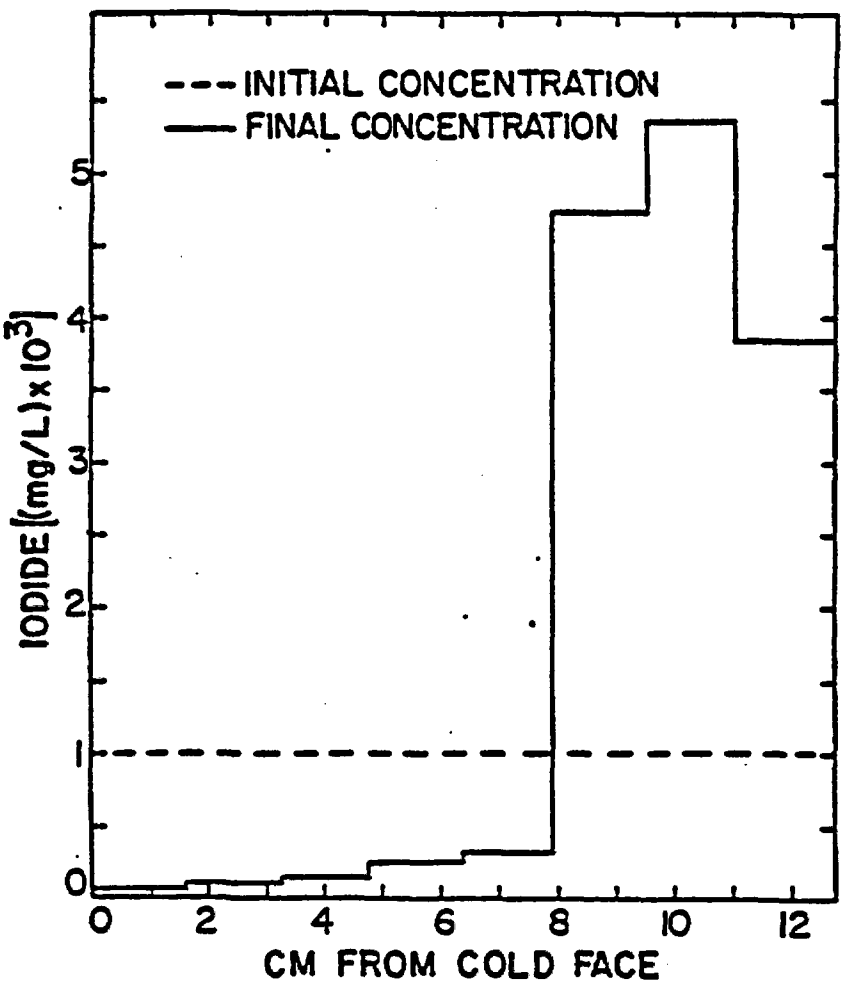

Figure 4.10 The change in iodide concentration in the pore solution within the nonwelded tuff core after heating horizontally.

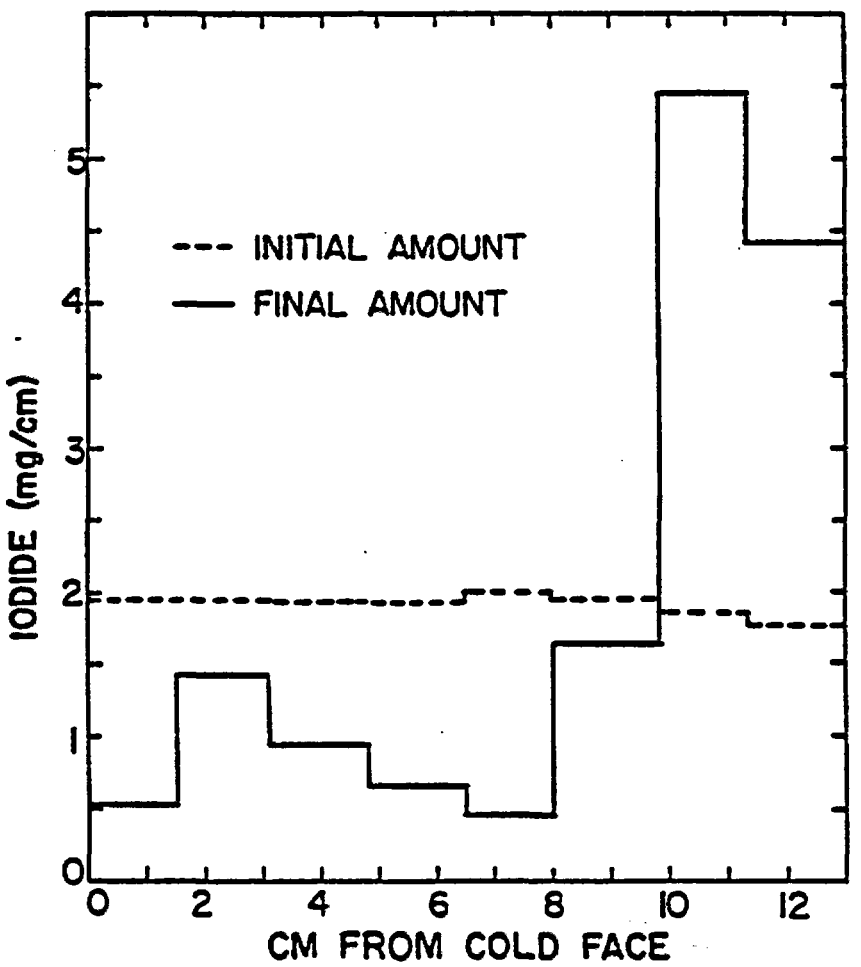

Figure 4.11 The change in the amount of iodide within each section of the nonwelded tuff core, which was heated horizontally.

porosity was 0.09. This porosity is much lower than the porosity of the nonwelded tuff. The discrete bulk densities at eleven 1-cm intervals are given in Figure 4.12. These are the average of 5 series of gamma measurements. The average of these 11 measurements was 2.435 gm/cm^3 with a range between 2.422 and 2.444 gm/cm^3. Thermocouples were installed between the core and the resevoir endplates.

The wetting of this core with iodide solution was more difficult than the wetting of the nonwelded tuff cores. After subjecting the core to negative pressure and adding the iodide solution, the core was allowed to soak in the solution for a week. The initial water content (Fig. 4.13) was higher at the ends of the core than in the center. This trait continued thoughout the heating. The welded tuff core was not desaturated after wetting. After soaking in the iodide solution, the water content was measured and the core was immediately sealed and attached to the heating apparatus. The level of saturation, about 58% saturation, was higher than the previous experiments.

The core was heated in a horizontal position for 32 days. The temperatures in the hot and cold reservoirs were 68.9° and 5.9°C, respectively. The temperatures between the aluminum endplates and the core were 65.7° and 8.5°C. The thermal gradient within the core was 4.7°C/cm. The steady-state thermal profile of the core is shown in Figure 4.14. The figure includes data from the five thermocouples inbedded in the core and the two measurements made between the core and the endplates.

The water content within the core was measured daily. Figure 4.13 shows the initial and final water content measurements. Data for

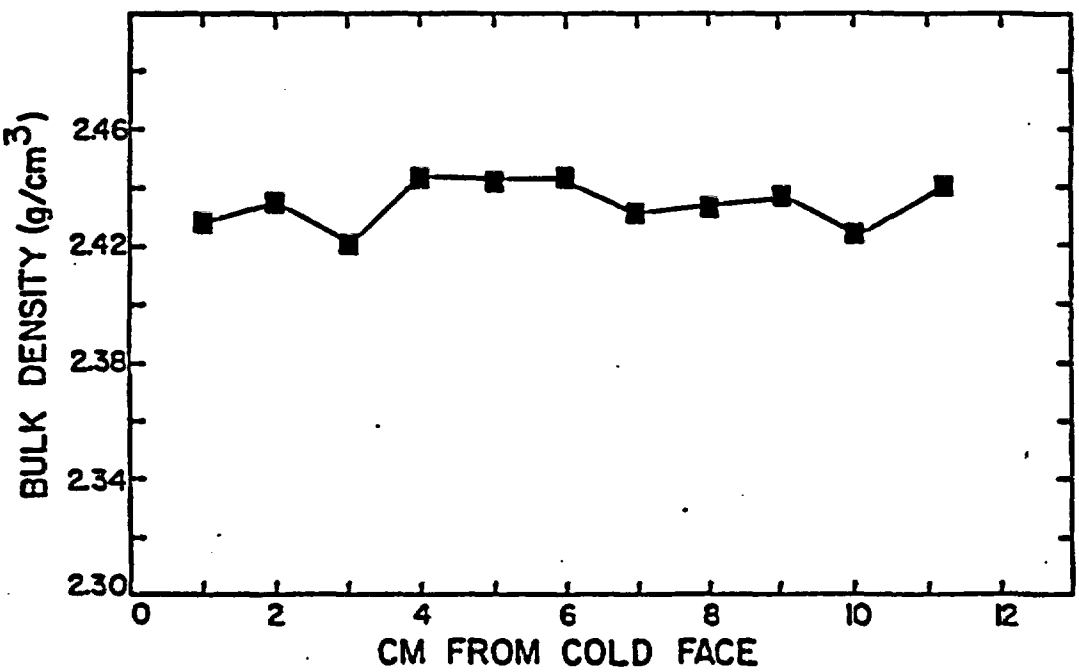

Figure 4.12 The dry bulk densities at eleven 1-cm intervals along the densely-welded tuff core.

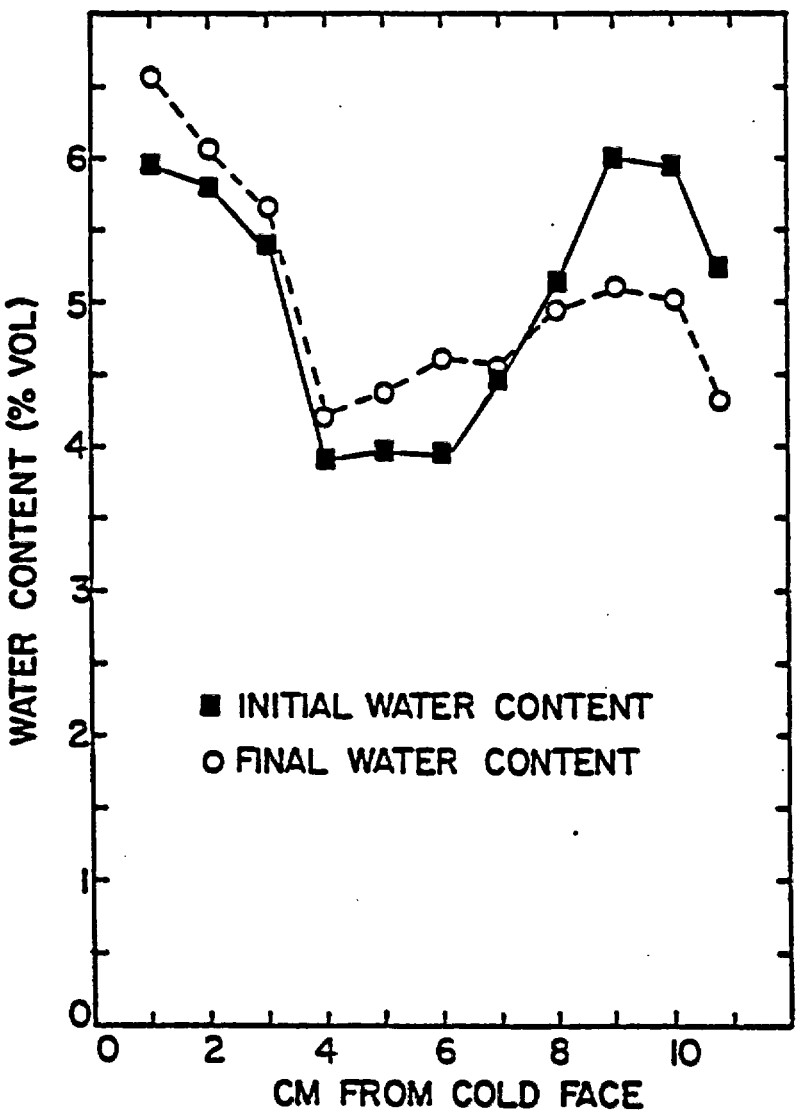

Figure 4.13 The initial and final water content of the densely-welded tuff core heated horizontally.

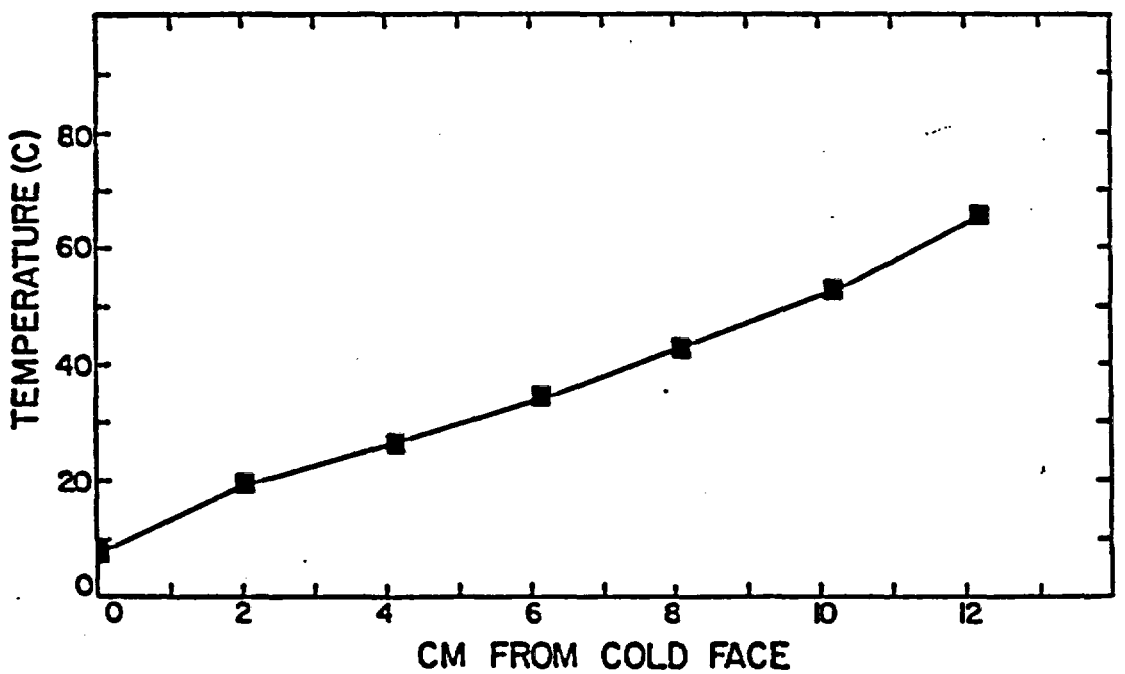

Figure 4.14 The temperature distribution within the densely-welded tuff core as it was heated in a horizontal position.

these and the intermediate water content measurements are given in Table 4.6. After heating, the core was cut into 6 slices, crushed and analyzed for iodide. The iodide analysis indicated that only about 60% of the iodide was recovered. Some iodide probably remained within the rock fragments. The analysis was adjusted so that a comparison could be made with the initial amount of iodide present in the core. This adjustment assumed that the percentage of iodide recovered in each core section was the same. Table 4.7 and Figures 4.15 and 4.16 show the results of the iodide analysis.

Discussion and Conclusion

The results of these heating experiments clearly show that countercurrent flow occurred in the tuff cores. The iodide analysis indicates that more liquid return flow occurred in the nonwelded tuff core samples than in the densely-welded tuff. The major factor controlling the liquid return flow is the unsaturated hydraulic conductivity of the cores. The time it took to wet the densely-welded tuff core indicates that it's conductivity is very low compared to the nonwelded tuff cores. This is to be expected because of the lower porosity of the welded tuff. More evidence of the low conductivity in the densely-welded unit is presented in the next chapter.

The amount of interconnected pore space within the cores is unknown. The degree of saturation achieved during the wetting of the nonwelded tuff cores indicated that the pore space was mostly interconnected. The welded tuff core may have had proportionally fewer interconnected pores than the nonwelded cores and, hence, less area

Table 4.6 Periodic water content measurements of the densely-welded tuff core as it was being heated horizontally.

CM FROM COLD FACE	1.00	2.00	3.00	4.00	5.00	6.00	7.00	8.00	9.00	10.00	11.00	Ave.
Initial H20 Cont.	5.97	5.79	5.39	3.91	3.96	3.95	4.46	5.14	6.02	5.96	5.23	5.07
Time After Heating												
Day 1	5.92	5.80	5.41	3.87	4.30	4.40	4.78	5.14	5.80	5.93	5.51	5.17
Day 2	6.18	5.84	5.40	3.84	4.36	4.39	4.66	5.08	5.77	5.86	5.24	5.12
Day 3	6.11	5.85	5.18	3.87	4.20	4.22	4.60	5.04	5.69	5.84	5.06	5.04
Day 4	6.35	5.80	5.30	3.78	4.22	4.62	4.49	4.98	5.45	5.70	5.26	5.08
Day 9	6.21	5.85	5.32	4.05	4.04	4.37	4.60	5.10	5.47	5.41	4.95	5.05
Day 10	6.12	5.53	5.17	3.94	4.04	4.17	4.19	5.14	5.24	5.24	4.60	4.87
Day 11	6.23	5.90	5.53	4.27	4.08	4.25	4.56	4.60	5.27	5.64	4.84	5.03
Day 12	6.06	5.90	4.40	3.86	4.18	4.16	4.16	5.04	5.34	5.34	4.66	4.92
Day 13	6.29	5.66	5.69	4.43	4.11	4.37	4.03	4.74	5.30	5.05	4.60	4.95
Day 14	5.90	6.03	5.40	4.10	4.17	4.31	4.74	5.00	5.29	5.39	4.31	4.97
Day 16	6.18	5.51	5.45	3.65	3.76	4.30	3.86	4.52	5.01	5.00	4.59	4.71
Day 17	6.20	5.64	5.63	3.89	4.24	4.30	4.02	4.51	4.94	5.11	4.23	4.79
Day 20	6.59	6.12	5.65	4.11	4.66	4.72	4.36	5.00	5.07	5.16	4.61	5.10
Day 22	6.63	5.55	5.71	4.17	4.50	4.64	4.21	4.61	4.81	4.99	4.24	4.93
Day 23	6.32	5.75	5.41	3.98	4.47	4.44	4.22	4.75	5.14	4.95	4.49	4.90
Day 24	6.66	6.14	5.63	4.22	4.55	4.37	4.40	4.74	5.02	4.90	4.22	4.99
Day 26	6.49	6.06	5.59	4.16	4.46	4.39	4.46	4.90	5.14	4.89	4.26	4.99
Day 27	6.66	6.04	5.76	4.16	4.53	4.46	4.45	4.84	4.84	5.03	4.37	5.02
Day 29	6.65	6.13	5.73	4.07	4.42	4.32	4.27	4.61	5.07	4.97	4.36	4.97
Day 30	6.58	6.06	5.66	4.22	4.36	4.61	4.55	4.95	5.11	5.02	4.30	5.04

Core section cm from cold side	0-2.25	2.25-4.33	4.33-6.4	6.4-8.26	8.26-10.26	10.26-12.2
Conc. I- (ppm)						
before heat	1000.00	1000.00	1000.00	1000.00	1000.00	1000.00
after heat	387.00	524.00	575.00	572.00	621.00	843.00
adjusted	645.00	873.00	959.00	953.00	1035.00	1405.00
Amount I- (ug/cm core)						
before heat	3.07	3.19	2.36	2.25	2.72	3.07
after heat	.95	1.46	1.46	1.38	1.84	3.00
adjusted	1.58	2.41	2.41	2.29	3.05	4.96

Table 4.7 The results of the iodide analysis for the densely-welded tuff core. Only 60% of the iodide was recovered during analysis. The adjusted figures indicate the iodide that would be present if it was fully recovered.

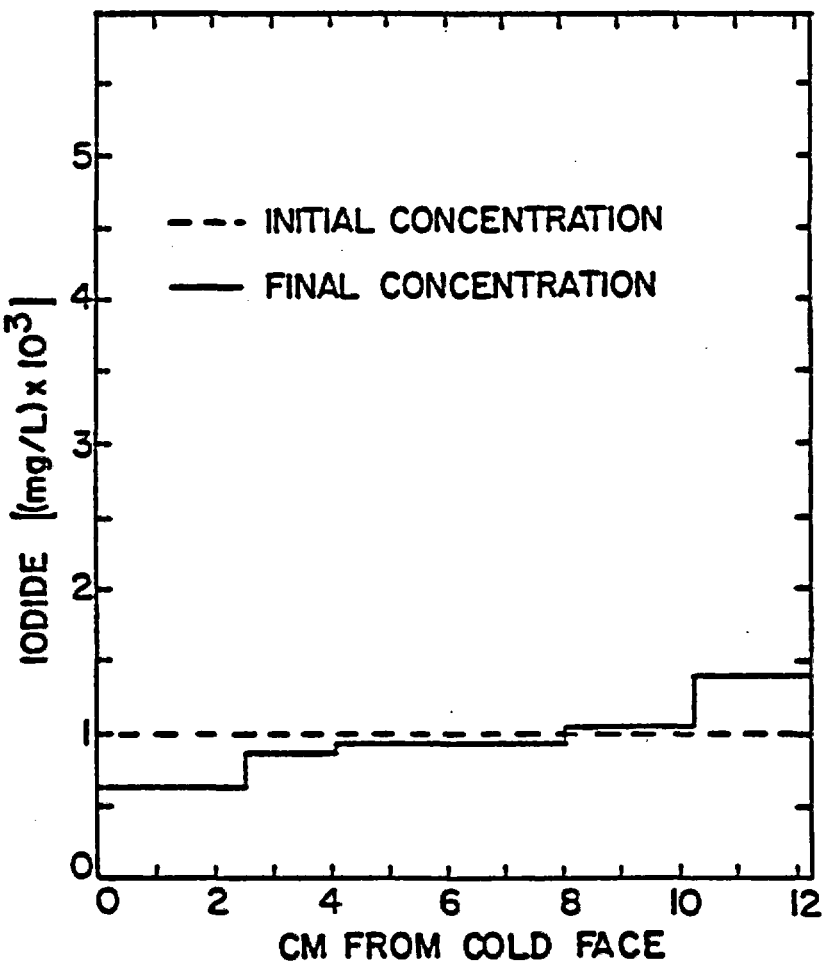

Figure 4.15 The change in concentration of iodide in the pore solution within the densely-welded tuff core. The concentration after heating is normalized (see Table 4.7).

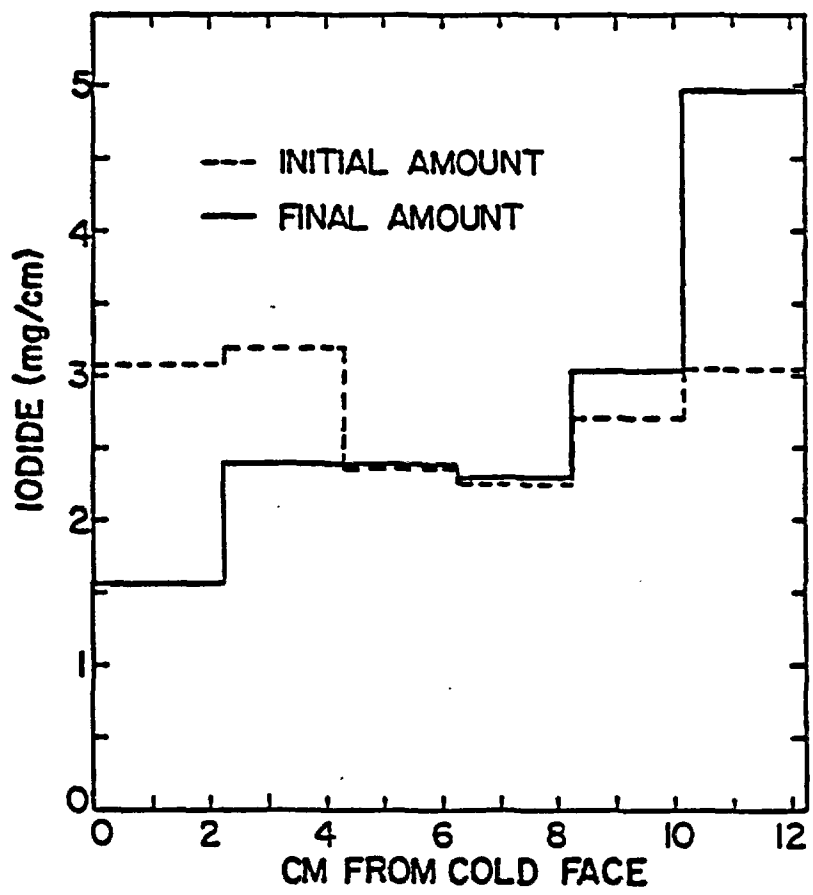

Figure 4.16 The change in the amount of iodide within the sections of the densely-welded tuff core. The amount after heating is normalized (see Table 4.7).

would be available for water movement than assumed by gravimetric porosity measurements. The hydraulic conductivity of the densely-welded tuff core would be reduced if this were true. Countercurrent flow is more pronounced at intermediate saturation levels. If the level of saturation is too high, vapor movement is restricted. If the level is too low, liquid return flow is retarded. The densely-welded tuff core started with a higher level of saturation than the nonwelded tuff cores. If some pore space was unavailable for water transport in the densely-welded tuff core, the effect would be that of an even higher saturation level. This could explain why less countercurrent flow occurred in the densely-welded tuff core compared to the nonwelded cores. The implication of this difference in water movement is important in a HLNW repository. A repository located in a layered volcanic formation will have differential flow in each layer which will depend on the individual properties of each layer. Studies of a particular repository site should attempt to find zones or beds with lower degrees of welding. These areas could contribute greater amounts of thermally driven water than would be expected using the average properties of the system.

Gravity flow is probably not a very important component of this system compared to flow caused by the potential gradient. The iodide analysis of the second experiment failed to show more liquid flow occurring in the lower half of the core. In the first experiment, reversing the gravity field failed to promote a greater liquid flow due

to gravity. The major component of the liquid return flow is probably the flow caused by the potential gradient.

A zone of soluble ions could be deposited within the dry, hot rock near the repository. These ions could remain in this zone until the repository cools enough to allow liquid water to return to this area. Escaping soluble radionuclides could be returned toward the repository by the liquid return flow system. The dimensions of the countercurrent flow system and the rate of moisture movement will depend upon the imposed thermal gradient, the initial water content and the hydrologic properties of the surrounding medium. The dimensions of this system could also be affected by any addition of water to the system, either meteorological or water escaping from the repository itself.

CHAPTER 5

FIELD HEATING EXPERIMENT

A field heating experiment was conducted in the densely-welded, fractured tuff at the Queen Creek road tunnel site (Fig. 3.2). The objectives of this experiment were to:

(1) Measure the changes in temperature caused by the addition of varied amounts of heat.

(2) Measure the changes in water potential and water content with time.

(3) Determine instrument and power requirements for future heating experiments.

Two nearly-parallel, horizontal boreholes (5 cm in diameter, 15 m long and 0.89 m apart), were used in this experiment (Fig. 5.1). A heating element was placed six meters into one borehole, while the adjacent hole was packed off at two locations to form an air space approximately the same distance into the borehole as the heater. Three thermocouple psychrometers were installed to monitor changes in water potential and temperature in the air space between the two packers. A neutron probe was used to determine changes in the water content of the tuff in both boreholes.

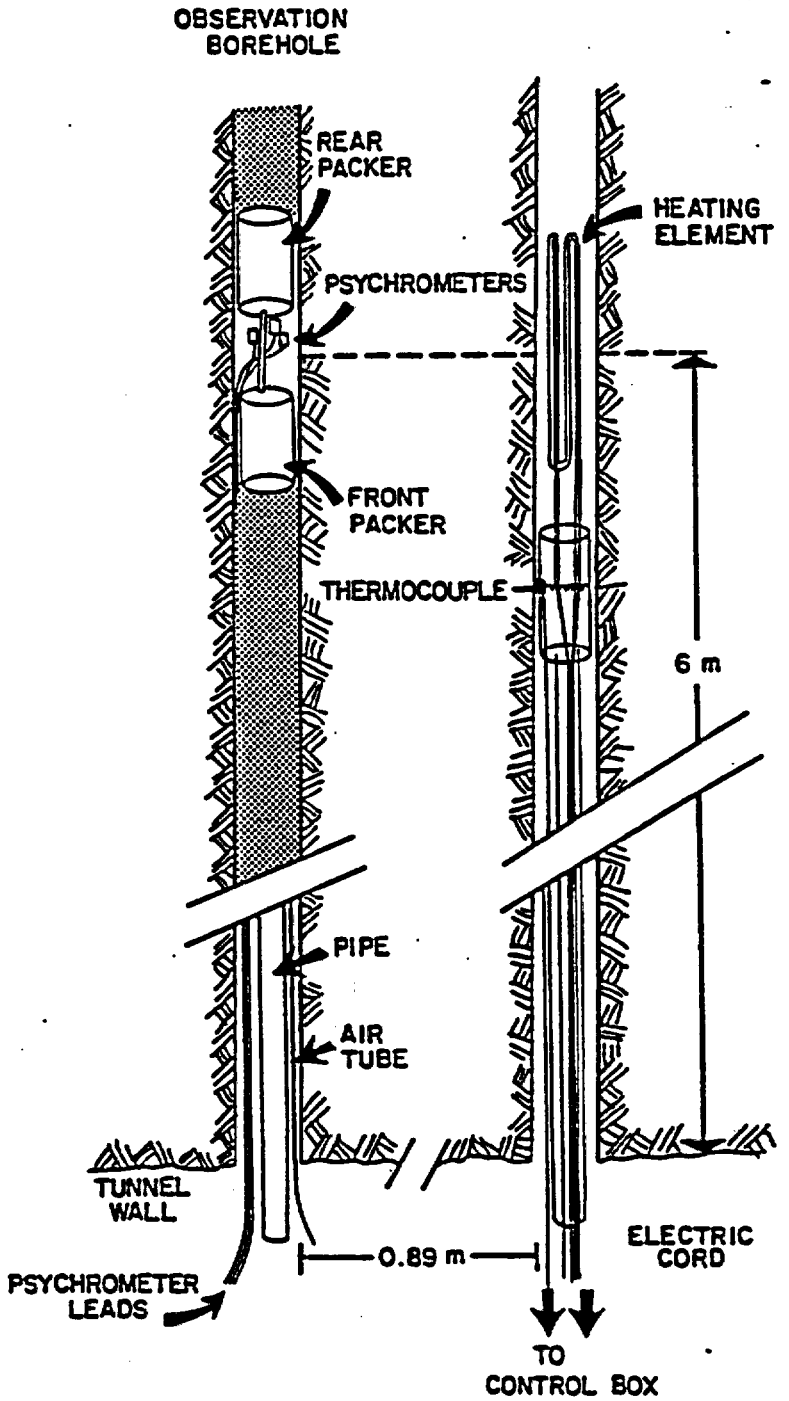

Figure 5.1 Diagram of the heating element and thermocouple (right borehole), and packers isolating psychrometers (left borehole) at the Queen Creek road tunnel site.

Experimental Setup

The heating elements used in this experiment are Incoloy 800 sheathed nickel alloy elements manufactured by W.W. Grainger Inc., Chicago, Illinois. The flange of each element was cut to fit into a combined temperature sensor and element holder (Fig. 5.2). The holder is 4.45 cm in diameter and holds the element in the borehole, preventing it from coming into contact with the rock. The elements normally use a 240 volt current at 60 hertz. While the elements were intended to be used submersed in a liquid, the application here required that they be used in air. Element burnout was avoided by reducing the voltage to 120 volts. This reduced the heat yield of each element to 1/4 of its potential output.

The two elements used are the 2000 and 6000-watt models, which effectively provide 500 and 1500-watt outputs for the experiments. The element lengths are 23.5 cm and 58.7 cm, respectively. The elements were powered by a field generator and controlled by a thermostat (Fig. 5.2), which monitored the temperature of the rock at a point midway along the heating element holder (Fig. 5.1). The thermostat can be adjusted between 100° and 200°C. Power was supplied by an electric cord running through a pipe to the element and connected to the thermostat control box. A thermocouple wire ran from the spring mechanism in the element holder, along the outside of the pipe, to the thermostat.

The thermocouple psychrometers used were manufactured by Wescor, Logan, Utah and are used in conjunction with a Wescor HR-33T dew point micro-voltmeter. Each psychrometer had been calibrated for different

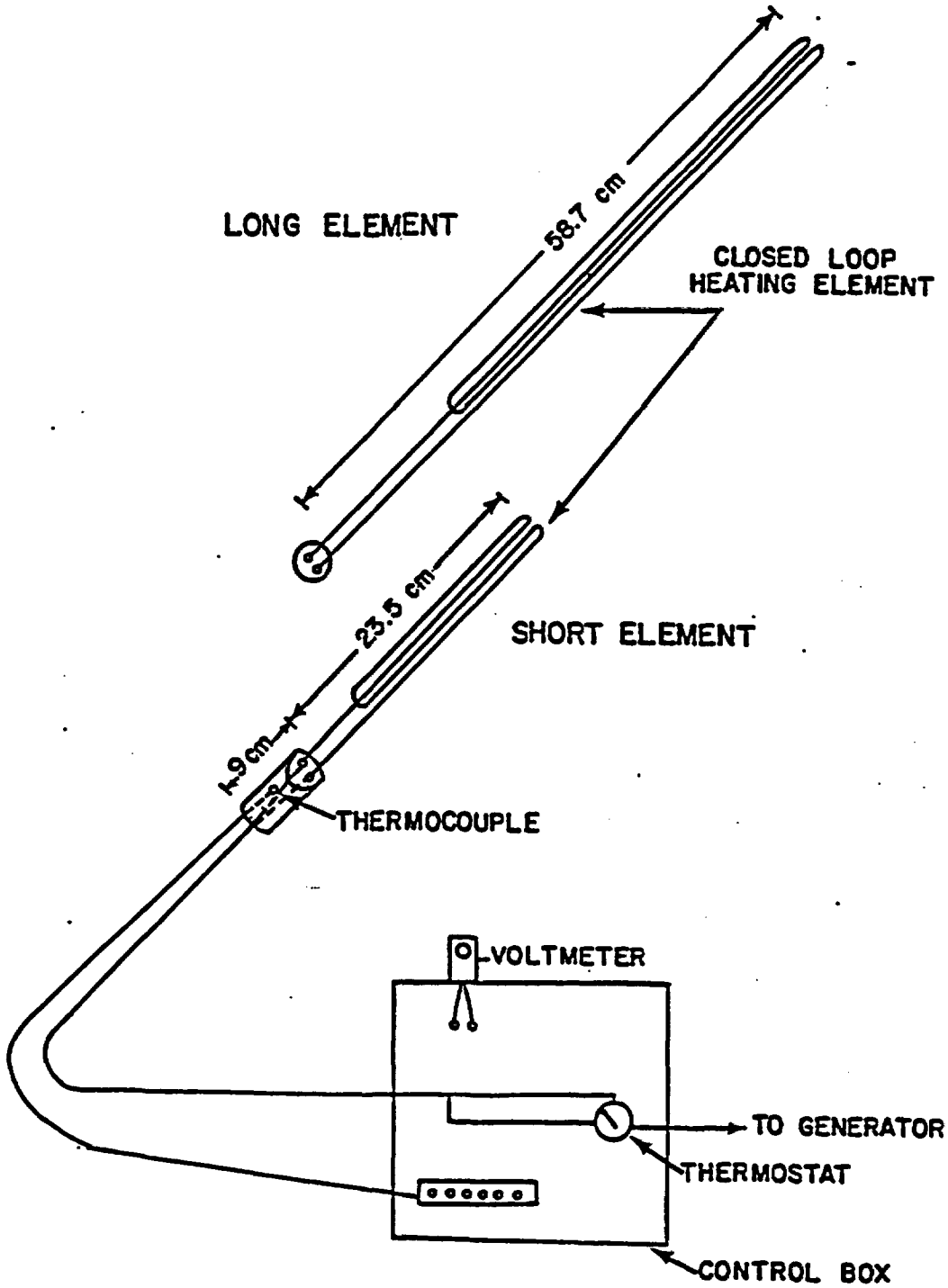

Figure 5.2 Diagram of the short (500 watt) and long (1500 watt) heating elements, and wiring chart to the control box.

temperatures and potentials. Two different methods, the dew point method and the psychrometric method, were used during calibration (see Wiebe et al., 1971). Calibration involved using salt solutions of varied concentrations to form different water potentials. The psychrometers were inserted into water tight chambers with one of the salt solutions. The chambers were lowered into a constant temperature water bath and allowed to equilibrate for 12 to 24 hours. Measurements were taken with the micro-voltmeter giving the voltage from each psychrometer at a particular temperature and potential. The temperature of the bath was then increased at 5°C intervals, between 15° and 35°C, and the psychrometers were allowed to re-equilibrate before another series of measurements was taken. For a more detailed discussion of the procedure used to calibrate psychrometers see Anderson (in preparation).

This procedure was followed with four different solutions, which gave potentials of 1.85, 9.44, 24.53 and 48.60 bars. Eight psychrometers were calibrated using this procedure. Each psychrometer had its own calibration curve. The three psychrometers that performed most consistently were used in the heating experiments. Only one psychrometer functioned properly throughout the heating experiment. Figure 5.3 is the calibration curve for that psychrometer.

Bulk water content within the tuff was measured using a neutron probe (Model 503, Hydroprobe, by Campbell Pacific Nuclear, Pacheo, California). The neutron probe measures the average water content within a spherical area around the probe. Therefore, sharp changes in water content cannot be determined with this method. At present no accurate calibration exists for this probe in a welded tuff. All data

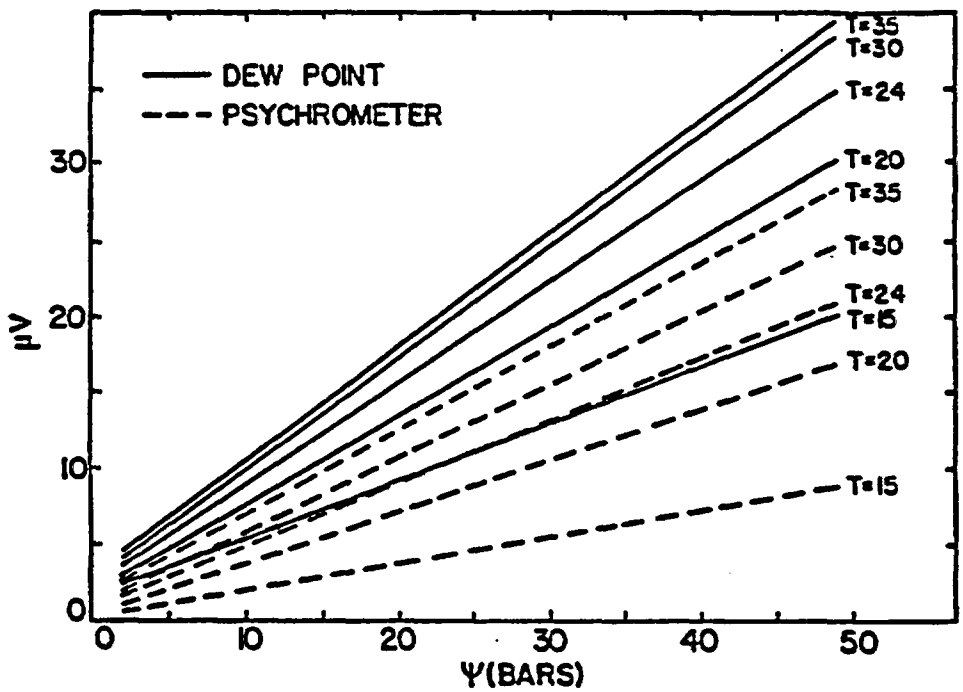

Figure 5.3 Calibration curve for the thermocouple psychrometer used in the field heating experiment.

are reported in the form of a ratio between the counts taken in the borehole and the shield count taken before each set of measurements. The ratio increases with increasing water content.

Experimental Procedure

The heating experiment was conducted in two parts. The first used the small 500-watt element. The second employed the larger 1500-watt element. The initial water content of the tuff was determined by taking three neutron probe measurements, over one-minute periods, at half-meter intervals in the two boreholes. The psychrometers were then installed six meters into the borehole between two packers and allowed to equilibrate for four days to determine the initial water potential. The heating element and the element holder were attached to a pipe and placed in the other borehole at a depth of six meters to the middle of the heating element.

Temperature and potential measurements in the observation borehole were taken hourly while the heater was operating. Heat was applied for approximately three days with the 500-watt element, then no heat was applied for four days. No change in the water potential was measured, so heat was again applied using the 1500-watt element for another four days. Neutron measurements were taken after heating to determine the change in water content. The thermocouple psychrometers and packers were removed after each heating period, neutron measurements were made, and the packers were replaced for periodic temperature and potential measurements. Periodic neutron measurements were also taken to monitor the recovery of the water content in the heated borehole.

Results and Discussion

In the first part of the experiment, the 500-watt element was emplaced and heated for 65 hours. The water content and water potential in the observation borehole did not change during this period, even though the temperature increased from 21.0° to 24.8°C. In the heater borehole, the water content decreased in the immediate vicinity of the heating element (Fig. 5.4). These results indicated that additional heat was required to obtain a sizable response in the observation borehole.

The psychrometers were left in place and a second heating trial was conducted, starting 103 hours after the first trial ended. During the time between the first and second heating episodes, the temperature in the observation borehole fell from 24.8° to 23.5°C and the water content in the heater borehole remained the same. In the second trial, the 1500-watt element was heated for 94 hours. In the observation borehole, the water potential decreased from approximately -0.25 to -9.0 bars. This change, and subsequent changes in potential after the element was turned off, are shown in Figure 5.5.

Data for water potential were obtained using the dew point method and the psychrometric method. The psychrometric method consistently indicated potential readings 0.5 to 1.5 bars below those determined using the dew point method. Data for Figure 5.5 were derived by averaging the potential values from the two methods. Psychrometers are not considered accurate at potentials greater than -2 bars and, therefore, the initial and final measurements only provide qualitative information about changes in water potential.

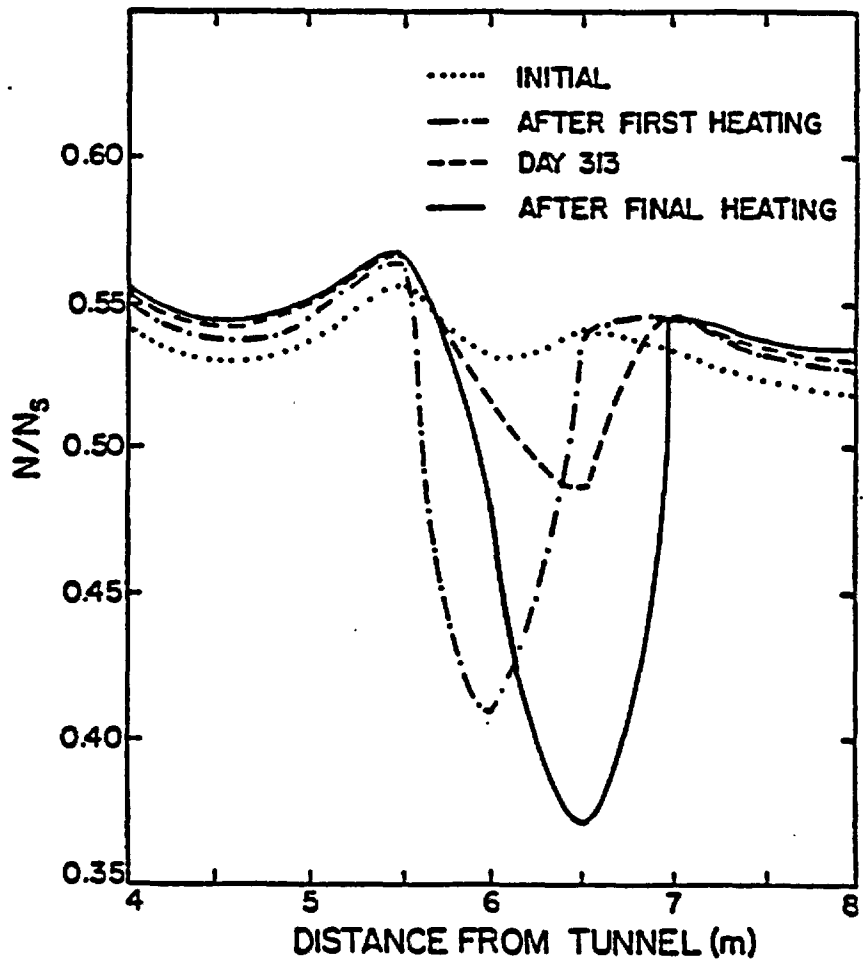

Figure 5.4 The change in water content, in the heater borehole, due to both the 500 and 1500 watt heating episodes. N is the average of three counts taken in the borehole and N_s is the average shield count.

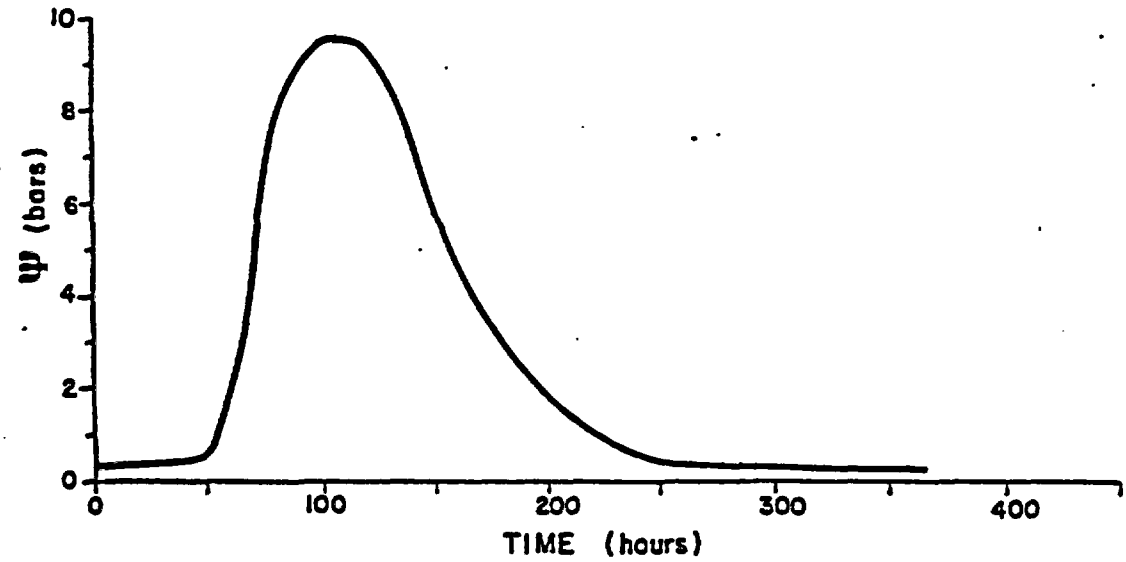

Figure 5.5 The change in water potential, in the observation borehole, due to the 1500 watt heating.

The temperature in the observation borehole increased durin time of heating, from 23.5° to 29.5°C (Fig.5.6). The temperature continued to rise for 28 hours after the heating was stopped, to 31. then gradually decreased. Temperature measurements taken in the hea borehole were made by the thermocouple, which was spring loaded in t element holder (Fig. 5.1). At that position, the temperature of the rock adjacent to the borehole increased to 90°C in 48 hours and continued to slowly rise after that to 91.5°C by the end of the heati period. The heating element was on continuously throughout the 94 ho heating period. The temperature never reached a level sufficient to trigger the thermostat mechanism.

After the heating was stopped, the temperature fell 9.9°C in t first 30 minutes of recovery. The sensor was then pushed further into the borehole and allowed to equilibrate. One hour after the heating, the temperature of the rock adjacent to the former heating element position was 132.3°C. This indicates that the temperature of the rock adjacent to the heating element was greater than the temperature measured by the sensor during heating. Two hours and 45 minutes after heating, the temperature at this position had dropped to 97.6°C.

During the second heating, the heating element was misposition by 0.36 meters, which resulted in the center of the element being located at 6.36 meters into the borehole instead of 6 meters. The results of this misplacement can be observed in Figure 5.4, which show the change in water content in the heater borehole after heating with the 1500-watt element. The results show an increase in the water content, during the second heating period, near the 6-meter depth.

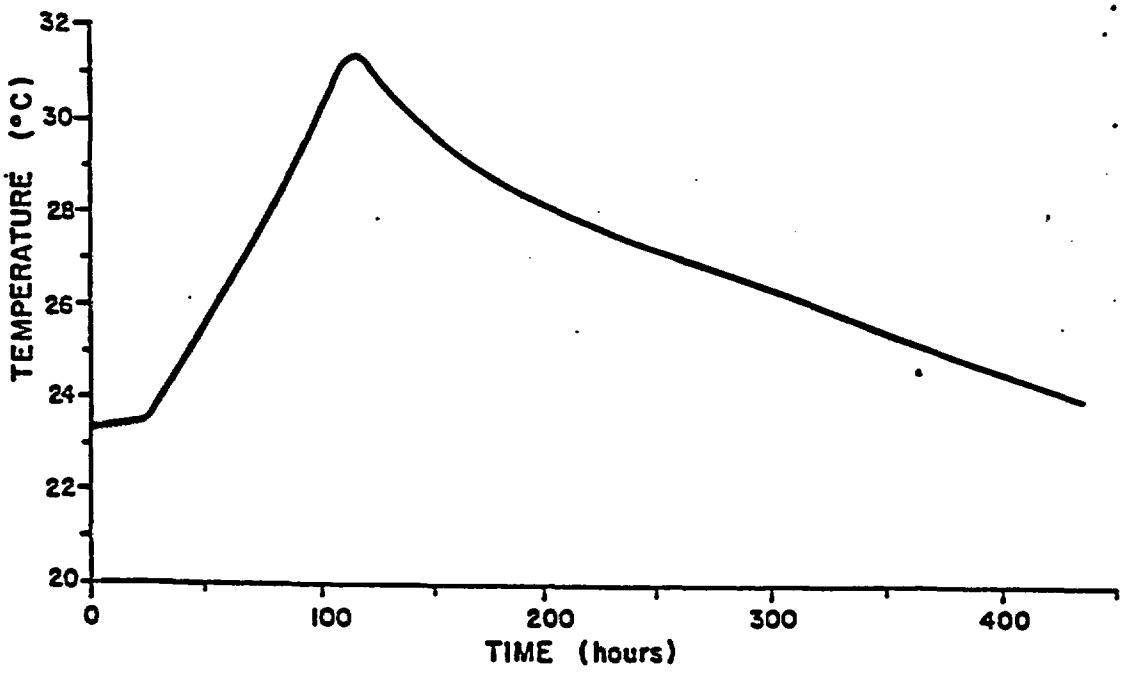

Figure 5.6 The temperature response, in the observation borehole, due to the 1500 watt heating episode. The element was heated for 94 hours.

Seven days after the heating was stopped, the temperature in the observation borehole had dropped to 27.0°C and the water potential had risen to near its initial state. Although the potential had decreased to approximately -9 bars during the second heating, no change in water content was observed. This indicates that a small change in water content can result in a large change in the potential for the range measured.

The recovery of the water content in the heater borehole was very slow (Table 5.1 and Fig. 5.4). Because wet and dry zones are located relatively close to each other (thus forming a large hydraulic gradient), the conclusion can be made that the hydraulic conductivity of the rock is low. Another factor in the slow recovery could be that some of the water left the system. During the heating, especially the second heating, liquid water dripped out of the heater borehole. This water would be unavailable to re-wet the dried area. Water was also ponded in the observation borehole behind the packer. This water flowed out of the borehole when the packers were removed to measure the water content with the neutron probe. The initial potential within the rock body indicates a high level of saturation. Water may have been forced into the boreholes to relieve the vapor pressure resulting from the heating. If the rock was initially near saturation, the water vapor may not have been able to diffuse through the small amount of air filled pore space.

Conclusions

This experiment was performed to determine thermally induced water movement in a large rock body. The 1500-watt heating element did

FIELD HEATING EXPERIMENT WATER CONTENT RECOVERY

Distance from tunnel wall (m)	4.0	4.5	5.0	5.5	6.0	6.5	7.0	7.5	8.0
Initial	.541	.528	.536	.557	.529	.537	.535	.521	.517
After first heat	.553	.536	.547	.564	.407	.542	.546	.531	.526
After second heat	.555	.543	.551	.566	.476	.370	.544	.530	.535
Recovery									
Day 71	.547	.539	.544	.561	.491	.410	.540	.529	.530
Day 114	.549	.539	.548	.565	.498	.435	.541	.534	.527
Day 198	.553	.541	.548	.564	.506	.466	.547	.531	.533
Day 313	.552	.541	.550	.568	.513	.486	.544	.535	.528

Table 5.1 The change in the water content within the heated borehole measured with a neutron probe. The numbers are the ratio between the counts taken in the borehole and the shield counts (see Fig. 5.4). Measurements were taken before and after each heating episode, and periodically during recovery.

induce water movement, but it is difficult to determine if most of the water left the system through the borehole, or if it was driven into the rock. Liquid water began to slowly drip out of the heater borehole, beginning four hours after the second heating commenced. It continued to leave the system throughout the heating phase of the experiment. Zones of low and high water content are adjacent to each other in the heater borehole. Yet the recovery of the water content within the rock will take over a year. This amount of time for recovery indicates that the hydraulic conductivity in the densely-welded tuff unit is very low.

The decrease in potential, measured in the observation borehole, indicated that a decrease in water content occurred there, but this decrease was too small to be measured with the neutron probe. A small water loss, then, can cause a large potential change within the densely-welded tuff. Heat from a HLNW repository could create quite large potential gradients if it were located in a similar rock formation. This effect would be beneficial if the dry zone remained confined within the rock formation. The potential gradient could cause liquid return flow to occur. Soluble radionuclides could be contained within the rock body by a countercurrent flow system.

Future heating experiments should have more instrumentation to determine the area affected by the addition of heat. Several observation boreholes at varying distances from the heater should be used. These boreholes could be instrumented at various depths to measure potential and temperature distributions. It would be desirable to seal all equipment in place with a material that has similar

hydraulic and thermal properties as the rock type involved. This would eliminate the ambiguity of water leaving the system. Multiple instrumentation is imperative. Although three psychrometers were used in this experiment, only one functioned properly throughout the experiment. Cased access holes could be used for neutron measurements to determine the water content without disturbing the flow system.

Finally, future experiments should be run with heating episodes, possibly with greater heat intensity, lasting for longer time periods. As shown in Figure 5.4, the recovery of the water content was very slow. In future experiments involving a larger affected area, this recovery could take years. Instrumentation should be designed to last for this amount of time.

THERMALLY INDUCED COUNTERCURRENT FLOW IN UNSATURATED ROCK

by

Daniel Wilson Matthews

A Thesis Submitted to the Faculty of the

DEPARTMENT OF HYDROLOGY AND WATER RESOURCES

In Partial Fulfillment of the Requirements
For the Degree of

MASTER OF SCIENCE
WITH A MAJOR IN HYDROLOGY

In the Graduate College

THE UNIVERSITY OF ARIZONA

1 9 8 6

RESULTS AND DISCUSSION

The results of laboratory heating experiments are presented and discussed below.

Sand Column Experiment Results

A simplified experiment to develop experimental techniques was run on a plexiglas column uniformly packed with washed silica sand. The average bulk density of the sand column was 1.5 gm/cm^3 (Table 4.1). The grain density of the sand was estimated to be 2.65 gm/cm^3. The average porosity of the sand column was estimated to be 43.4 percent. The initial water content of the column was estimated gravimetrically at 3.4 percent. The water content at a point near the cold face of the sand column increased from 3.4 percent by volume to 7.7 percent in nine days (Figure 4.1 and Table 4.1). The water content at points near the heated end of the sand column decreased from 3.4 percent to nearly zero water content in the same time period. Water content increased steadily during the experiment near the cold face (Figure 4.2). Water content decreased and effectively dropped to zero to a point 10.2 cm from the cold face. An apparent steady state was attained after nine days of heating.

Table 4.1. Sand column heating experiment.

Distance From Cold End (cm)	Dry Bulk Density (gm/cm^3)	Initial Water Content (percent)	Water Content (percent)			
			Day 2	Day 4	Day 5	Day 9
1.2	1.51	3.4	4.4	6.3	6.1	7.8
2.2	1.55	3.4	3.7	5.7	5.6	7.7
3.2	1.56	3.4	3.7	5.4	6.1	6.5
4.2	1.52	3.4	3.5	4.6	5.2	6.2
5.2	1.55	3.4	3.8	5.1	5.3	4.8
6.2	1.55	3.4	3.6	4.7	5.0	4.6
7.2	1.53	3.4	3.6	4.0	4.4	3.7
8.2	1.51	3.4	3.7	3.1	2.9	3.9
9.2	1.56	3.4	2.9	2.9	2.5	2.2
10.2	1.52	3.4	2.3	0.8	0.0	0.0

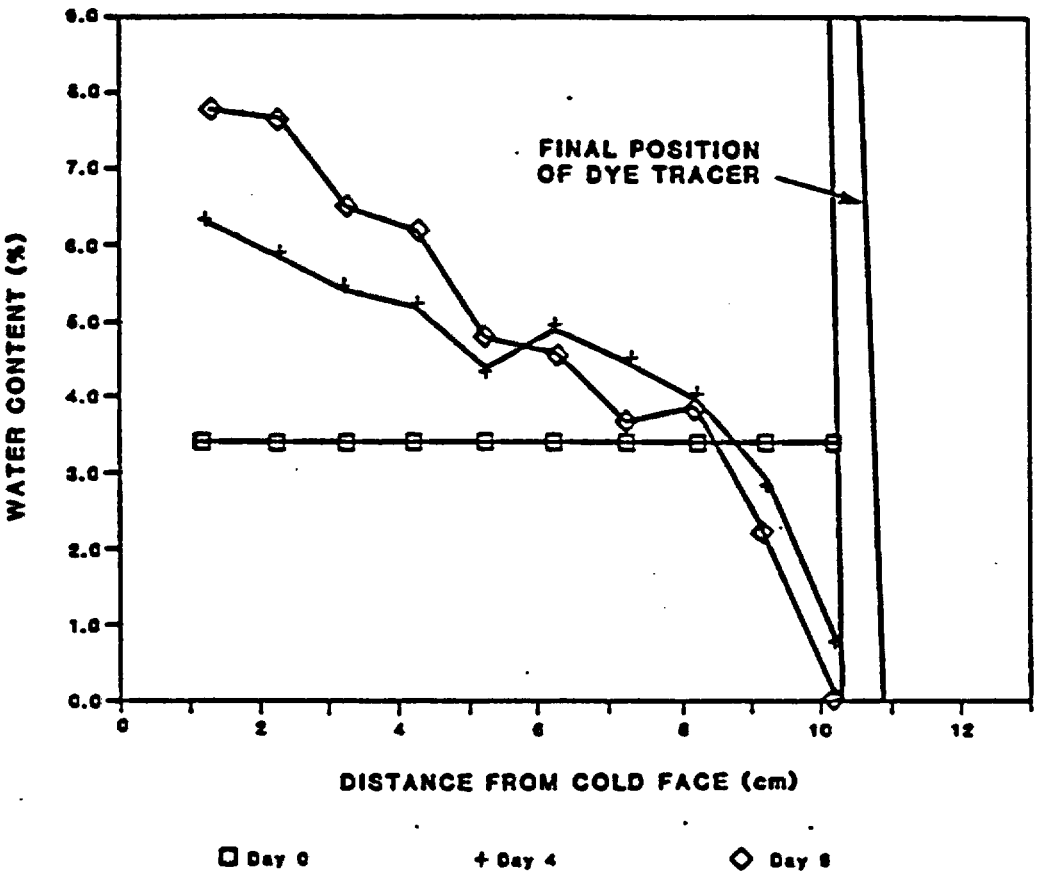

Figure 4.1. Sand column heating experiment water content along axis of column.

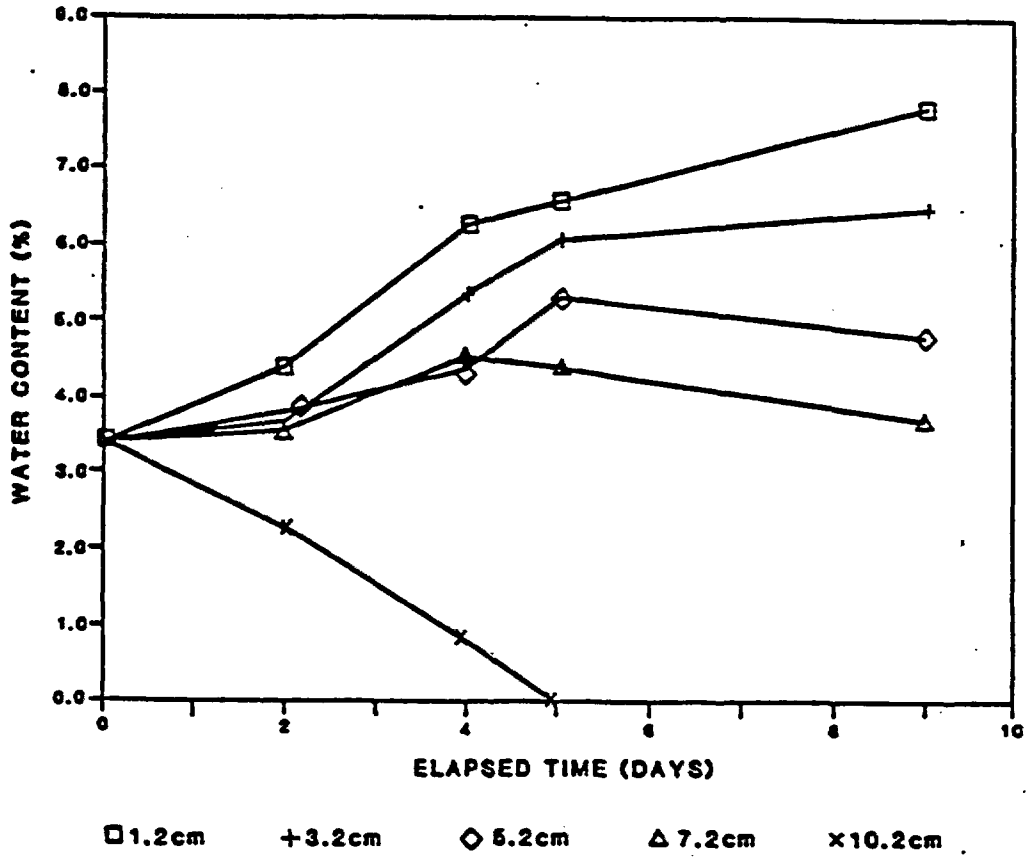

Figure 4.2. Sand column heating experiment water content changes with time and distance from cold face.

Figure 4.1 shows that an essentially dry zone was created in the sand column extending 2.5-cm from the hot face of the column. Liquid water return flow deposited tracer in a darkened disk where the liquid flow intersected the dry zone created by vapor movement away from the heat source. The disk was concave towards the cold end. The concavity of the disk implies that the vapor flux was greater at the central axis of the sand column because the dry zone was extended there. This suggests that the axial temperature gradient was reduced at the edge of the column and implies that there was a substantial radial temperature gradient in the sand column.

The visible intensity of the ink disk was greatest at the circumference of the sand column indicating that substantial radial flow occurred, contrary to previous assumptions about the one-dimensional nature of the flow system. The endplate reservoirs at the hot and cold ends were maintained at temperatures of 40°C and 20°C, respectively, so that the average temperature in the core was approximately 30°C. Radial temperature gradients in the column, and consequently radial vapor flow may be reduced by limiting the average temperature in the test cores to near the ambient laboratory temperature of 22°C. The temperatures in the endplate reservoirs at the hot and cold ends of the test setup were maintained at approximately 40°C and 2°C, respectively, in subsequent experiments.

The ink disk was tilted in the vertical plane with the lower edge 0.5 cm closer to the hot face of the sand column. The force of gravity will tend to produce a convection cell with vapor rising to the top of the horizontal column and flowing towards the cold end. The vapor condenses at the cold end of the column and the liquid sinks. Liquid water return flow along the bottom of the column completes the cycle. A vertical convection cell operating in the sand column would tend to enhance the axial vapor flux along the top of the horizontal column causing the dry zone to extend further from the hot face. This may indicate that gravitational effects on moisture movement were not negligible in this experiment.

Sandstone Core Experiment Results

The sandstone core reached steady state after twelve days of heating. The average temperature gradient was 2.2°C/cm with a maximum temperature of about 36°C in the core. The bulk density of the core averaged 2.15 gm/cm^3 (Table 4.2). The grain density of the sandstone was estimated to be 2.54 gm/cm^3. The average porosity of the sandstone core was estimated to be 15.3 percent by volume. The initial water content ranged from 2 percent to 10 percent, Figure 4.3. Figure 4.4 shows the difference in volumetric water content between the intact core and sections of that core prepared following the experimental

Table 4.2. Sandstone core heating experiment.

Distance From Cold End (cm)	Dry Bulk Density (gm/cm^3)	Initial Water Content (percent)	Water Content (percent)									
			Day 1	Day 3	Day 5	Day 7	Day 9	Day 11	Day 13	Day 14	Day 15	Day 16
1	2.18	7.3	8.8	8.4	8.2	8.4	9.8	8.7	9.1	8.8	8.8	9.2
1.5	2.12	9.9	9.6	9.7	9.7	9.4	9.7	9.6	10.0	10.3	10.1	9.9
2.5	2.13	8.8	8.8	9.0	9.6	8.8	9.5	9.0	10.4	10.8	10.3	9.8
3.5	2.10	7.5	7.6	8.9	9.3	8.1	8.7	8.4	9.2	9.6	9.2	9.0
4.5	2.08	7.9	7.9	7.9	7.9	7.7	7.6	7.6	7.6	7.8	7.5	7.3
5.5	2.11	5.3	5.5	5.3	5.4	5.4	5.4	5.4	5.2	5.2	5.0	5.0
6.5	2.15	5.4	5.1	5.0	4.9	5.0	4.9	4.8	4.9	4.9	4.8	5.0
7.5	2.20	3.8	3.4	3.3	3.6	3.6	3.3	3.4	3.4	3.4	3.3	3.4
8.5	2.11	2.4	2.6	2.1	2.4	2.5	2.5	2.4	2.2	2.5	2.4	2.1
9.5	2.09	4.1	2.8	2.6	2.9	2.8	2.6	2.5	2.5	2.5	2.5	2.6
10.5	2.09	4.8	3.7	3.2	3.6	3.6	3.4	3.4	3.2	3.3	3.3	3.3
11.5	2.10	5.1	4.0	3.2	3.7	3.6	3.5	3.3	3.2	3.2	3.1	3.1

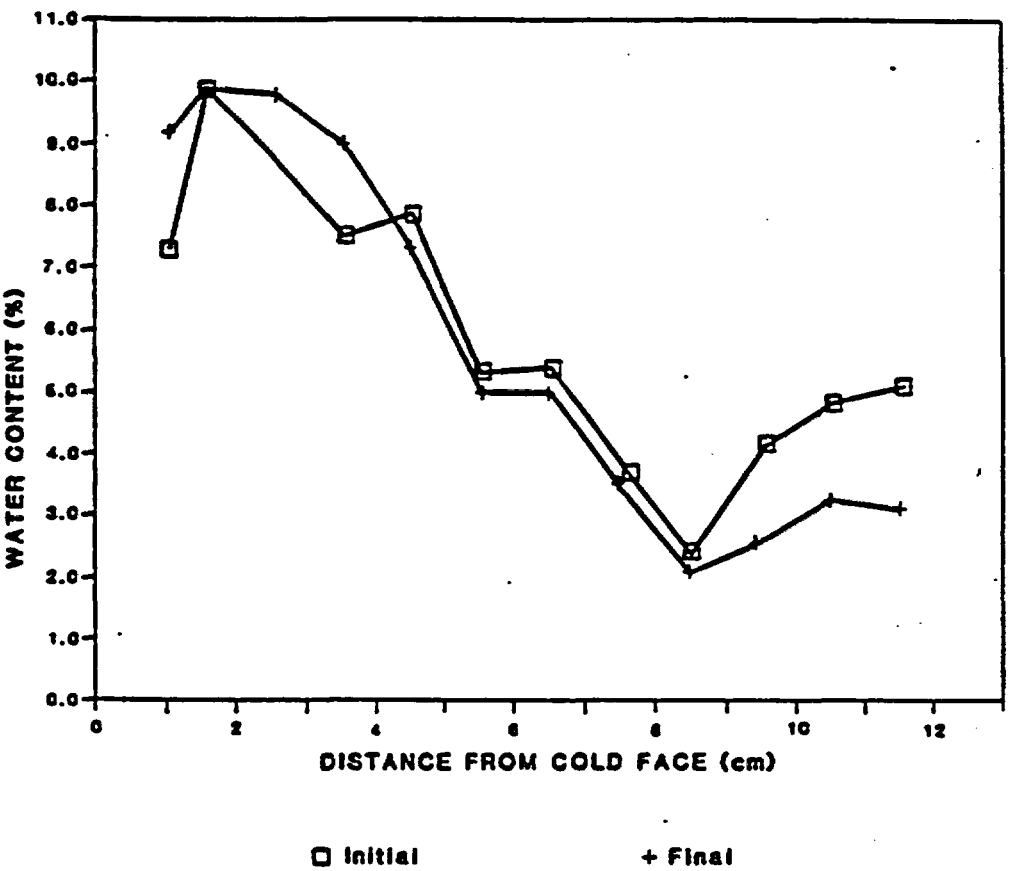

Figure 4.3. Sandstone core heating experiment initial and final water content distribution.

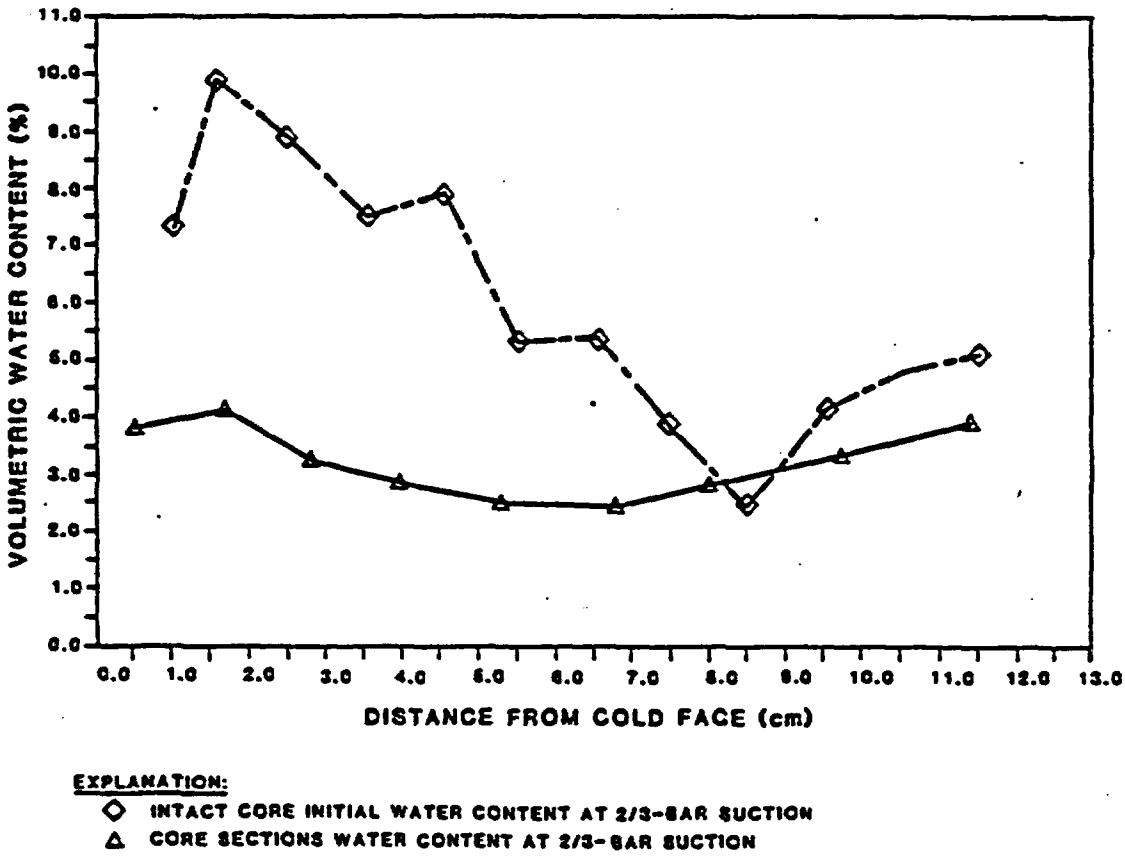

Figure 4.4. Sandstone water content in intact core and core sections at 2/3-bar suction.

run and equilibrated on a porous ceramic plate at the same pressure, 2/3-bar. The intact core retained more water with much more variation in water content than did small slices of that core. This indicates that the saturated rock core was not equilibrated long enough in the porous plate moisture extractor to obtain a uniform initial water content. Water content decreased from 4.7 percent to 2.7 percent at a point near the hot face of the sandstone core while water content increased from 7.3 percent to 9 percent at a point near the cold face (Figure 4.3 and Table 4.2).

Water content decreased during the experiment at a point 11.5-cm from the cold face, stabilizing after twelve days of heating (Figure 4.5). Water content increased at a point 1.0-cm from the cold face with decreases in water content between the first and the fifth days and between the ninth and the eleventh days. Water content near the mid-point of the core remained stable throughout the experiment.

The initial concentration of fluorescein tracer in the solution used to saturate the sandstone core was 6.0 ppm. No fluorescein tracer was visible in room light or under ultraviolet light on the surface exposed when the core was cut in half lengthwise at the end of the experiment. The ranking of filtrate from the crushed core sections is shown in Figure 4.6. The initial tracer distribution in the core was assumed to correlate exactly with the initial water content distribution and is represented by a plot of the

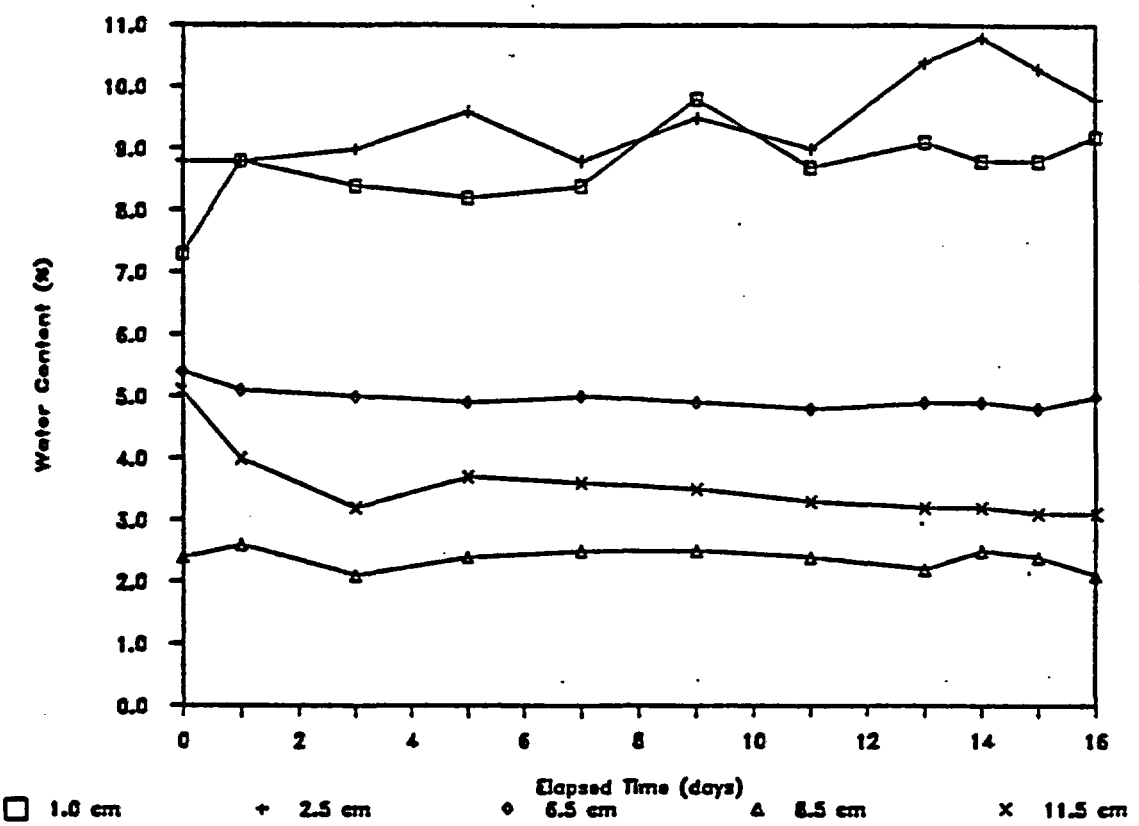

Figure 4.5. Sandstone core heating experiment water content changes with time.

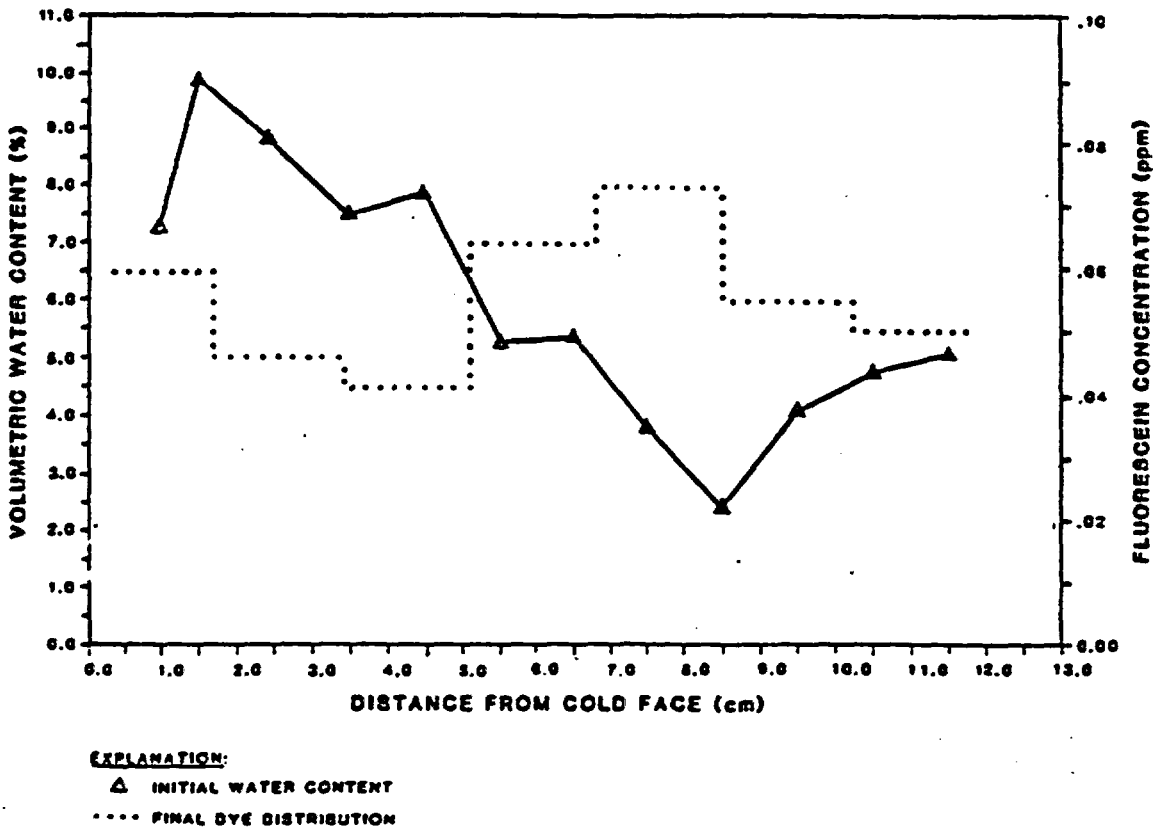

Figure 4.6. Sandstone core tracer distribution.

initial water content distribution in the sandstone cylinder. The concentration of the tracer in the filtrate was less than 0.1 ppm, indicating that the tracer may have adsorbed to the core.

Figure 4.6 shows that the final tracer concentration was lowest 2 to 5 cm from the cold face and highest in a zone extending from 5 to 8.5 cm from the cold face. The final tracer distribution indicates that liquid water return flow carried the tracer from cold to warm until an apparent obstruction to flow was encountered 8.5 cm from the cold face. Figure 4.3 shows that a relatively dry zone existed in the initial water content distribution in the core. This suggests that liquid water flowed from the cold face toward the hot face and that the liquid water return flow may have been limited by a low permeability zone resulting from the low initial water content 8.5 cm from the cold face.

Tuff Core Experiment Results

The final heating experiment was conducted on a sealed tuff cylinder subjected to an average temperature gradient of 2.22°C/cm. The bulk density of the core averaged 2.34 gm/cm^3 (Table 4.3). The grain density was estimated to be 2.53 gm/cm^3. The porosity of the tuff core was estimated to be 7.5 percent by volume. The water content of the five small disks cut from the same tuff sample averaged 10.4 percent with a standard deviation of

Table 4.3. Tuff core heating experiment.

Distance From Cold End (cm)	Dry Bulk Density (gm/cm^3)	Initial Water Content (percent)	Water Content (percent)								
			Day 1	Day 5	Day 7	Day 11	Day 14	Day 16	Day 19	Day 20	Day 21
0.5	2.35	8.7	9.7	8.6	8.3	9.3	9.2	9.5	9.3	9.4	9.3
1.5	2.34	6.9	7.3	6.6	6.0	6.7	6.5	6.3	7.3	7.4	6.9
2.5	2.34	7.1	6.8	6.2	5.7	6.2	5.9	5.9	6.3	6.3	5.9
3.5	2.33	7.8	7.0	6.7	6.2	6.1	5.7	5.6	5.8	5.7	5.6
4.5	2.33	7.3	6.1	5.1	4.7	4.8	4.5	4.5	4.5	4.6	4.4
5.5	2.33	7.0	5.5	5.0	4.0	3.9	3.7	3.5	3.8	3.8	3.6
6.5	2.34	5.7	4.1	2.6	2.3	2.0	1.9	1.9	2.0	2.0	1.9
7.5	2.35	4.7	3.3	2.3	1.6	1.5	1.4	1.2	1.4	1.4	1.2
8.5	2.33	6.4	5.3	4.1	3.7	3.7	3.6	3.4	3.4	3.5	3.4
9.5	2.35	6.1	4.3	3.4	2.8	2.7	2.4	2.5	2.6	2.5	2.5
10.5	2.35	7.7	7.3	6.2	5.7	5.5	5.5	5.5	5.7	5.4	5.5
11.5	2.35	7.5	8.4	7.0	6.7	6.6	6.5	6.3	6.3	6.3	6.3

0.2 percent water content. The range in the initial water content in the large core was greater than that of the small slices equilibrated at the same pressure, (1-bar) implying that the core may not have had enough time to reach equilibrium when it was removed from the moisture extractor device. Initial and final water content distributions are shown in Figure 4.7. The initial water content is substantially higher than the final water content at all points along the core, indicating that water diffused out of the "sealed" core. Figure 4.8 shows that the water content in the tuff core decreased steadily throughout the experiment except at a point 0.5-cm from the cold face. The water content at that point decreased between the first and the seventh days then increased to a stable value of approximately 9.3 percent. A quasi-steady state was attained after 16 days of heating. The diffusion of water across the plastic compound used to seal the cores may have been substantial over that time period.

The water content change is expected to be greatest near the hot face. The calculated decrease in water content during the experiment at the hot end of the core, 12 cm from the cold face, was similar to the decrease of approximately 2 percent near the the middle of the core, 7 cm from the cold face (Figure 4.7). This suggests that liquid water return flow reduced the water content change at the hot face. The decrease in the water content 0.5 cm from the

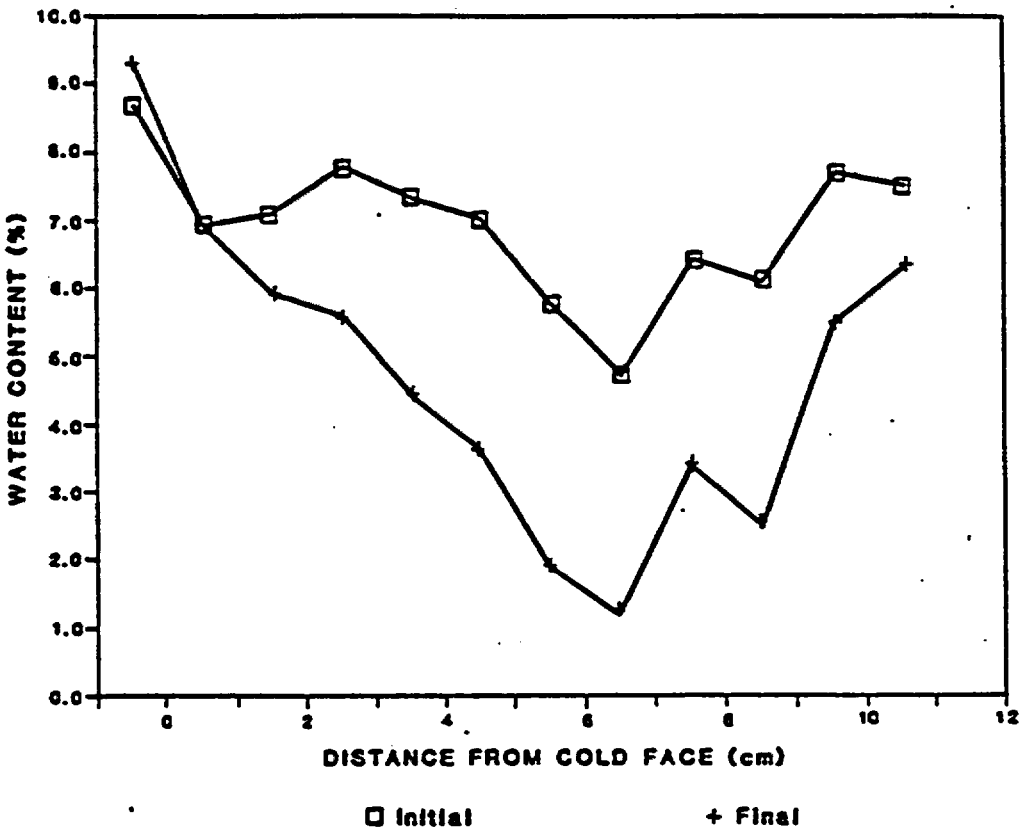

Figure 4.7. Tuff core heating experiment initial and final water content distribution.

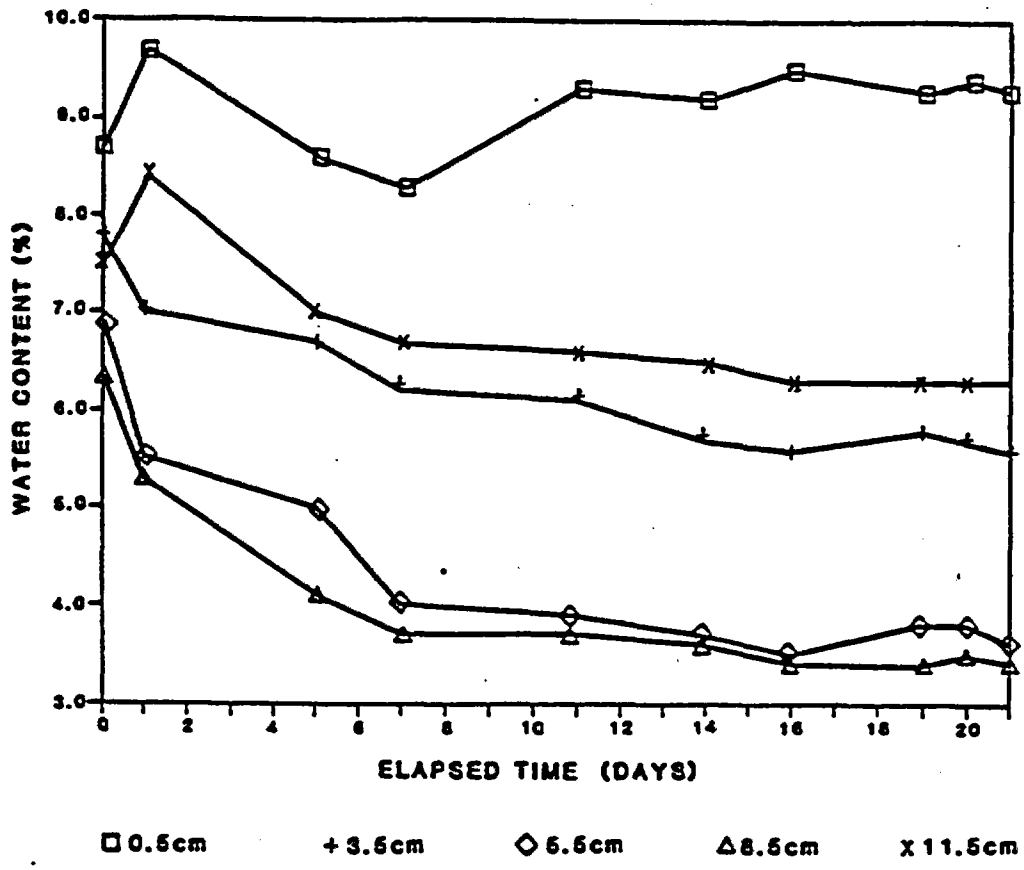

Figure 4.8. Tuff core heating experiment water content changes with time.

cold face of approximately 0.5 percent was less than that observed at any other location along the axis of the core. This indicates that vapor flow from the hot end towards the cold end of the tuff cylinder reduced the water content change at the cold face.

Rock Core Temperature Gradients

The axial temperature data (Figure 4.9) for the tuff core fit a straight line, indicating a uniform temperature gradient was established in the core. The thermal conductivity of the tuff matrix is greater than that of water or air (Wang et al. 1983). Also the water and air filled pore space of this welded tuff core amounted to less than 8 percent of the volume of the core. Latent heat transport would increase the apparent thermal conductivity of the rock core near the hot end where liquid water was vaporized, and decrease the apparent thermal conductivity of the rock core near the cold end, compared to the center of the core. As a result the temperature gradient should have been progressively lower closer to the hot end of the core if latent heat transport was a significant heat transport process in the tuff core. The linearity of the axial temperature data suggests that heat conduction through the solid tuff was the dominant heat transport process.

The axial temperature data (Figure 4.9) for the sandstone core indicated that the temperature gradient was

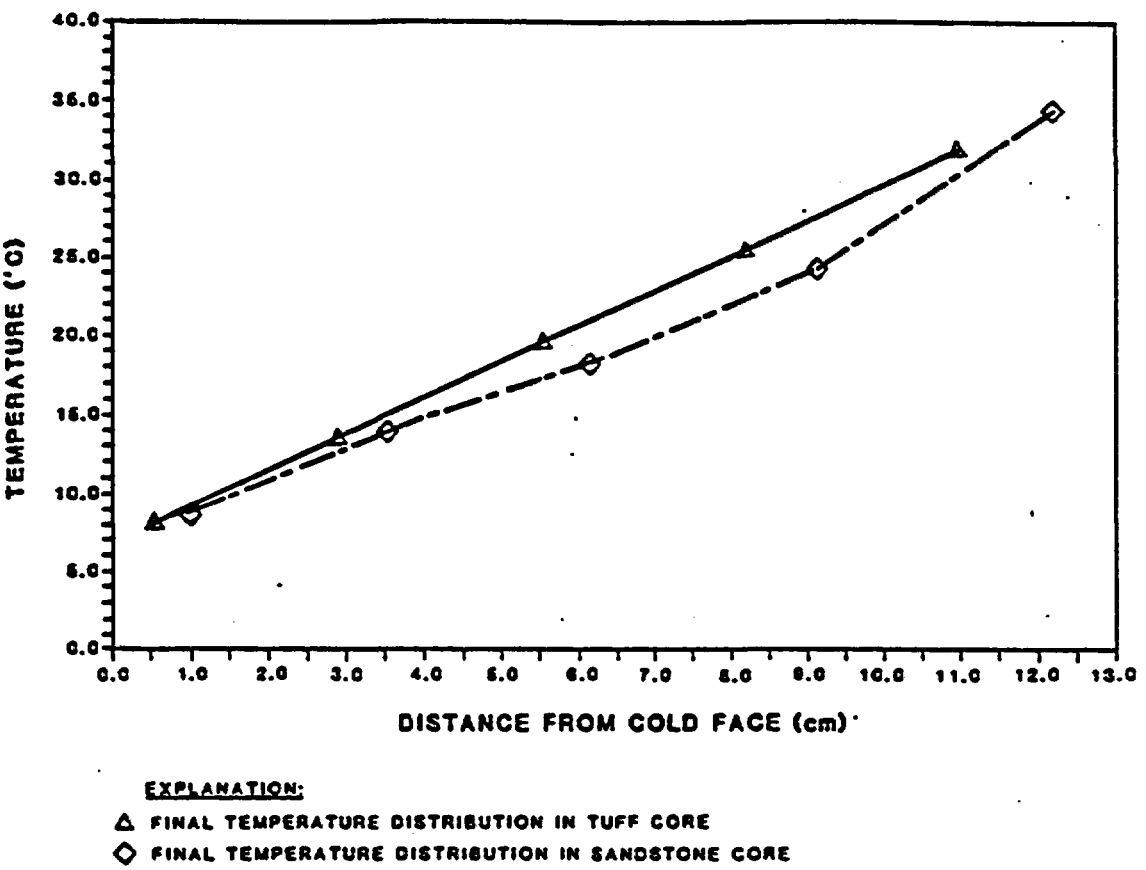

Figure 4.9. Temperature distribution at the end of tuff and sandstone heating experiments.

steeper near the hot end of the core and less steep near the cold end of the core compared to the center of the core. The potential for latent heat transport was significantly greater in the sandstone core because the proportion of water and air-filled pore space (15.3 percent by volume) was approximately twice that of the tuff core. The greater water content near the cold end increased the thermal conductivity of the core (and reduced the temperature gradient) close to the cold end. The apparent thermal conductivity near the hot end was less than the apparent thermal conductivity near the center of the core because the water content was lower. These results suggest that heat conduction through the water and air-filled pore space contributed significantly to heat transfer in the sandstone core. Latent heat transfer may have been limited by the relatively low temperatures in the core (less than the boiling point of water at atmospheric pressure).